UNIVERSIDADE ESTADUAL PAULISTA
"JÚLIO DE MESQUITA FILHO"
Câmpus de São José do Rio Preto

Bianca Gottardo de Almeida

# One-Pot Synthesis and Antifungal Activity of Non-Toxic Silver-Hydroxyapatite Nanocomposites against *Candida* Species

São José do Rio Preto
2018

Bianca Gottardo de Almeida

# One-Pot Synthesis and Antifungal Activity of Non-Toxic Silver-Hydroxyapatite Nanocomposites against *Candida* Species

Dissertação apresentada como parte dos requisitos para obtenção do título de Mestre em Microbiologia, junto ao Programa de Pós-Graduação em Microbiologia, do Instituto de Biociências, Letras e Ciências Exatas da Universidade Estadual Paulista "Júlio de Mesquita Filho", Câmpus de São José do Rio Preto.

Financiadora: CAPES

Orientador: Prof. Dr. Diogo Paschoalini Volanti

São José do Rio Preto
2018

A447o

Almeida, Bianca Gottardo de
One-pot synthesis and antifungal activity of non-toxic silver-hydroxyapatite nanocomposites against Candida species / Bianca Gottardo de Almeida. -- São José do Rio Preto, 2018
54 f. : il., tabs.

Dissertação (mestrado) - Universidade Estadual Paulista (Unesp), Instituto de Biociências Letras e Ciências Exatas, São José do Rio Preto
Orientador: Diogo Paschoalini Volanti

1. materiais nanoestruturados. 2. síntese. 3. Candida spp. 4. concentração inibitória mínima. 5. micoses. I. Título.

Sistema de geração automática de fichas catalográficas da Unesp. Biblioteca do Instituto de Biociências Letras e Ciências Exatas, São José do Rio Preto. Dados fornecidos pelo autor(a).

Essa ficha não pode ser modificada.

Bianca Gottardo de Almeida

# One-Pot Synthesis and Antifungal Activity of Non-Toxic Silver-Hydroxyapatite Nanocomposites against *Candida* Species

Dissertação apresentada como parte dos requisitos para obtenção do título de Mestre em Microbiologia, junto ao Programa de Pós-Graduação em Microbiologia, do Instituto de Biociências, Letras e Ciências Exatas da Universidade Estadual Paulista "Júlio de Mesquita Filho", Câmpus de São José do Rio Preto.

Financiadora: CAPES

Comissão Examinadora

Prof. Dr. Diogo Paschoalini Volanti
UNESP– Instituto de Biociências, Letras e Ciências Exatas da Universidade Estadual Paulista "Julio de Mesquita Filho", *Campus* São José do Rio Preto.
Orientador

Prof[a]. Dr[a]. Carolina Colombelli Pacca
UNESP– Instituto de Biociências, Letras e Ciências Exatas da Universidade Estadual Paulista "Julio de Mesquita Filho", *Campus* São José do Rio Preto.

Prof[a]. Dr[a]. Márcia Maria Costa Nunes Soares
Instituto Adolfo Lutz - Laboratório de São José do Rio Preto

São José do Rio Preto
19 de dezembro de 2018

## AGRADECIMENTOS

O presente trabalho foi realizado com apoio da Coordenação de Aperfeiçoamento de Pessoal de Nível Superior - Brasil (CAPES) - Código de Financiamento 001.

## RESUMO

O impacto de doenças fúngicas e a resistência aos agentes antimicrobianos por fungos patogênicos tornou-se um desafio global para a saúde da população. No presente trabalho, a síntese de nanocompósitos a base de prata-hidroxiapatita (Ag-HAP), foram sintetizados por um método solvotérmico assistido por micro-ondas com diferentes concentrações de peso de prata, testadas contra espécies de *Candida* sensíveis e resistentes aos azólicos comumente utilizado na plática clínica. Estudos antifúngicos foram conduzidos por método de microdiluição – seguindo o protocolo M27 A3 - CLSI. Para todas as espécies de *Candida* testadas, a amostra Ag pura mostrou baixa atividade antifúngica quando comparada com as amostras combinadas de Ag-HAP, com claro efeito sinérgico, uma vez que a atividade antifúngica foi molhorada quando colocados juntos. O principal efeito inibitório foi observado em Ag4%-HAP e Ag8%-HAP contra *Candida krusei*, com concentração inibitória mínima (CIM) de 31,2µg / mL, seguido por *Candida parapsilosis stricto sensu* (62,5 µg / mL), *Candida tropicalis*, (62,5 µg / mL), *Candida glabrata* (125 µg / mL) e *Candida albicans* (125 µg / mL). Além disso, ensaios toxicicológicos foram realizados com modelo *in vivo*, *Galleria mellonella* devido à similaridade de resposta imunológica e níveis de toxicidade entre mamíferos. O teste foi executado de duas maneiras: banho e inoculação de todos os nanocompósitos, com a mesma concentração utilizada nos testes de microdiluição. Todos NCs não apresentaram toxicidade para este modelo. A atividade antifúngica específica encontrada por aanálise quantitativa demonstra que os nanocompósitos agem de forma diferente conforme os alvos, considerando espécies de *Candida*. Estes resultados mostram um novo potencial antifúngico para aplicações tecnológicas e *coatings.*



Palavras-chave: materiais nanoestruturados, síntese, *Candida* spp*,* concentração inibitória mínima, micoses.

## ABSTRACT

The impact of fungal diseases and the battle for antimicrobial agents against pathogenic fungi has emerged as a main global healthcare challenge. Here, the antifungal activity of silver-hydroxyapatite (Ag-HAP) nanocomposites (NCs) with different Ag concentrations synthesized by the one-pot microwave-assisted solvothermal method was evaluated against sensitive and resistant *Candida* species. Antifungal studies were conducted by microdilution method – protocol from the Clinical and Laboratory Standard Institute. The main inhibitory effect was seen to Ag4%-HAP against *Candida krusei*, with minimum inhibitory concentration (MIC) of 31.2 µg/mL, followed by *Candida parapsilosis* Sensu Stricto (62.5 µg/mL)*, Candida tropicalis,* (62.5 µg/mL), *Candida glabrata* (125 µg/mL) and *Candida albicans* (125 µg/mL). Furthermore, the toxicity assay was performed in the *in vivo* model *Galleria mellonella*. The test was executed by bathing or inoculating with the same NCs concentration used in the previous microdilution tests. For both approaches, all NCs concentrations were not toxic to *G. mellonella*. The specific antifungal activity demonstrates that NCs act efficiently against species of *Candida*. These results show a potential antifungal application for well-designed nanostructured Ag-HAP composites.

.



Keywords: nanostructured materials, one-pot synthesis, *Candida* spp, minimum inhibitory concentration, mycoses.

**SUMÁRIO**

# CAPÍTULO 1

## 1 – INTRODUÇÃO E REVISÃO DE LITERATURA

Nas últimas décadas, infecções relacionadas aos fungos, mesmo que não sejam tão frequentes quanto às bacterianas ou virais, têm recebido especial atenção pelo aumento do número de novos casos (HUFFNAGLE; NOVERR, 2013; NETEA et al., 2015). Estima-se que, mundialmente, 1,7 bilhão de indivíduos estão acometidos por algum tipo de infecção fúngica, que varia desde superficiais até invasivas, podendo ser de caráter agudo a crônico (SPITZER; ROBBINS; WRIGHT, 2017). O número de mortes anuais associadas a esses tipos de infecções fúngicas é de mais de 1,5 milhão, sendo similar às taxas de mortalidade relacionadas à tuberculose e três vezes mais do que a da malária (BONGOMIN et al., 2017).

A maior parte dos processos infecciosos ocasionados por fungos são de natureza oportunista, ou seja, ocorrem quando há um déficit no sistema imunológico do hospedeiro. Outros fatores, como: tratamento com quimioterápicos, transplante de órgãos, uso dispositivos médicos sintéticos, doenças de base como lúpus e diabetes, entre outros, podem ser fatores predisponentes para desencadear a patogênese fúngica (BROWN et al., 2012).

Dentre a variedade de micro-organismos potencialmente patogênicos, destaca-se a *Candida*. Este gênero leveduriforme composto por aproximadamente 200 espécies é amplamente disperso na natureza e faz parte da microbiota humana típica, presente, por exemplo, na cavidade bucal, orofaringe, pele, mucosa vaginal, secreções brônquicas, urina e fezes (MAYER; WILSON; HUBE, 2013). No âmbito hospitalar, é o microrganismo mais comum de infecção fúngica. Neste contexto, as espécies mais frequentes são: *C. albicans*, *C. glabrata*, *C. tropicalis*, *C. parapsilosis* e *C. krusei* (WHALEY et al., 2017).

*Candida albicans* ainda é a espécie mais frequente, o que é evidenciado por estudos nos Estados Unidos, Europa e Oriente Médio (CLEVELAND et al., 2015; KLINGSPOR et al., 2015; SHARIFZADEH et al., 2013). Fatores de virulência, tais como: dimorfismo, expressão de adesinas e invasinas na

superfície celular, formação de biofilmes, e secreção de enzimas hidrolíticas, são características desse espécie (KULLBERG; ARENDRUP, 2011).

A incidência de infecções causadas por espécies de *Candida* não-albicans vem aumentando constantemente nos últimos anos. Importantes diferenças geográficas na distribuição dessas espécies e padrões de suscetibilidade antifúngica, *in vitro,* podem ser observados (Figura 1) (PAPPAS et al., 2018).

Figura 1 – Variações geográficas na distribuição de espécies de *Candida*. Globalmente, *Candida albicans* é a espécie mais prevalente associada com candidíase invasiva; no entanto, a distribuição de *Candida* não-albicans pode variar, como demonstrado na figura. Dados são apresentados da Austrália, Brasil, Canadá, Dinamarca, França, Japão e Estados Unidos.

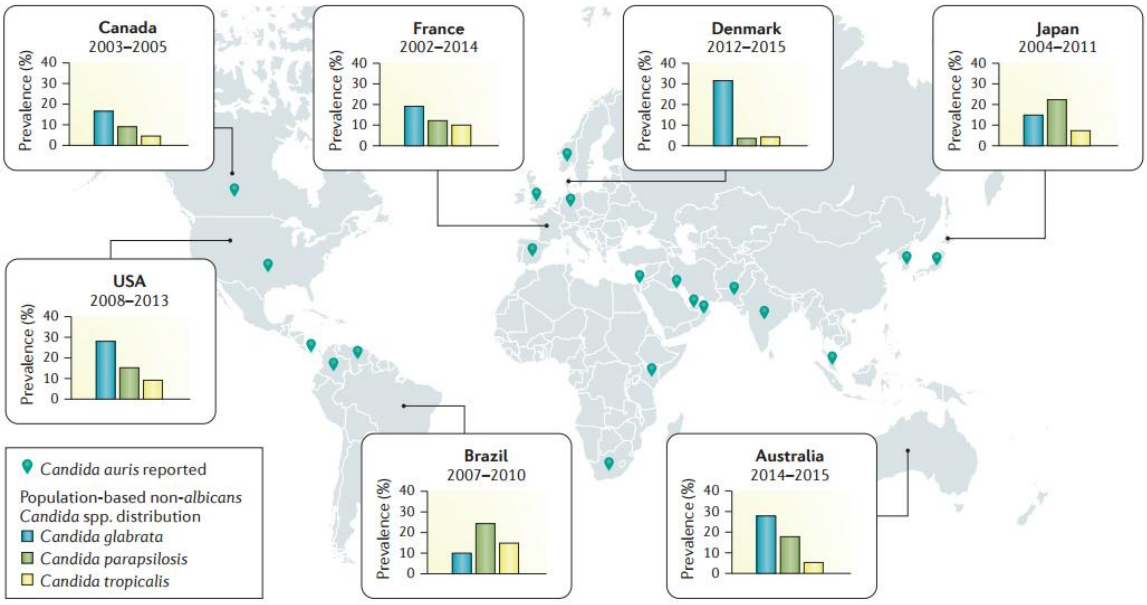


Fonte: Pappas et al. 2018.

Atualmente, há um grande problema relacionado ao tratamento dessas infecções, uma vez que as drogas disponíveis tem custos elevados, e apresentam efeitos tóxicos aos pacientes. Além disso, a administração de doses inadequadas pode promover a seleção de cepas resistentes (SANTOS et al., 2018). Muitos estudos documentaram a capacidade dessas espécies em desenvolver alta resistência aos azólicos, classes mais comuns de antifúngicos utilizados na prática clínica (LOPEZ-RIBOT et al., 2017), cujo mecanismo de ação envolve o bloqueio da síntese do ergosterol, importante constituinte da membrana celular dos fungos (SANTOS et al., 2018).

Na maioria das infecções por *C. albicans*, o antifúngico mais comumente prescrito é o fluconazol (PAUL; MOYE-ROWLEY, 2014; WHALEY et al., 2017) no entanto, diversos mecanismos de resistência são observados, sendo a regulação do gene ERG e bomba de efluxo mediadores-chave da resistência a essa classe de fármacos (FLOWERS et al., 2012).

Algumas das espécies não-albicans, como *C. glabrata* e *C. krusei*, frequentemente apresentam perfis de resistência aos antifúngicos (DIEKEMA et al., 2012). *Candida glabrata*, por exemplo, possui a capacidade de absorver esteróis exógenos e crescer com esteróis que não sejam o ergosterol na membrana celular. Esse mecanismo permite a evasão do micro-organismo frente ao tratamento com azol, adquirindo assim, resistência (WHALEY et al., 2017).

Já a *Candida krusei* é intrinsecamente resistente ao fluconazol, embora o mecanismo preciso ainda não é totalmente compreendido. Vários estudos têm atribuído a resistência intrínseca de *C. krusei* aos azólicos à atividade de bomba de efluxo e reduzida acumulação do fármaco (KATIYAR; EDLIND, 2001)(LAMPING et al., 2009). Azólicos mais recentes, como o voriconazol, possuem atividade fungicida em frente a *C. krusei*; no entanto, perfis de resistência também já foram reportados (KRISHNASAMY et al., 2018; RICARDO et al., 2014)

Em relação a ação de *C. tropicalis* e *C. parapsilosis*, elas são naturalmente suscetíveis a maioria dos agentes antifúngicos. No entanto, a resistência adquirida pode ocorrer, especialmente para o fluconazol (XIAO et al., 2015).

Com relação a outros antifúngicos, apenas uma nova classe foi introduzida nos últimos 30 anos, as equinocandinas (SPITZER; ROBBINS; WRIGHT, 2017). No entanto, resistência a essa classe também já foi relatada em *Candida* (WHALEY et al., 2017).

Diante do exposto, a busca por alternativas eficazes e viáveis aos medicamentos antimicrobianos tradicionais torna-se extremamente relevante. No cenário atual, pesquisas por novas estratégias de combate e controle de doenças microbianas buscam por novas fontes de moléculas bioativas, que exerçam sua ação, com poucos efeitos colaterais (BEYTH et al., 2017;

FERNANDO; GUNASEKARA; HOLTON, 2018; LAKSHMINARAYANAN et al., 2018).

A nanotecnologia está relacionada à caracterização, produção e aplicações de estruturas, dispositivos e sistemas, controlando-se a forma e o tamanho em escala nanométrica. Com sua popularização, nanopartículas (NPs) podem ser sintetizadas de variadas formas a fim de atingir o produto de acordo com sua aplicabilidade, como por exemplo na agricultura, microeletrônica, biomedicina. (AARTHI et al., 2018; KUMAR; YADAV, 2009; LARA et al., 2018)

Baseado nisso, sistemas nanoestruturados, tais como, nanopartículas poliméricas, nanoemulsões, nanopartículas lipídicas sólidas, lipossomas e cristais líquidos, são capazes de promover a liberação e veiculação de princípios bioativos com atividade antimicrobiana (QIN et al., 2017). A aplicabilidade destes sistemas de liberação de fármacos, além de otimizar a solubilização de compostos, podem potencializar a ação terapêutica dos mesmos (CHERAGHI et al., 2017). Suas vantagens sobre fármacos convencionais também incluem seu tamanho reduzido, diferentes mecanismos de ação, redução de toxicidade e alta biocompatibilidade (GONZÁLEZ et al., 2018). Quando combinadas com NPs de prata (Ag), por exemplo, esses compostos têm demonstrado alta atividade em relação ao controle de doenças bacterianas e fúngicas (XIE et al., 2014). Esses compostos, quando associados à hidroxiapatita (HAP, [$Ca_5(PO_4)_3(OH)$]), por ser um componente natural da estrutura dos ossos e dentes, aumentam a biocompatibilidade, podendo ser uma alternativa viável para tratamento de infecções, inclusive aquelas causadas por micro-organismos resistentes (MOCANU et al., 2014; XIONG et al., 2016).

Estudos correlacionando nanopartículas de prata (como potente antimicrobiano), combinado a outros compostos (hidroxiapatita, grafeno, ouro) têm sido alvo de investigação, com diferentes formas de sínteses e objetivos de aplicação.

Mocanu et al. (2014) sintetizaram uma hidroxiapatita complexa com nanopartículas de zinco, prata e ouro, para revestimento de implantes ortopédicos e dentários ou utilizados como cimentos ósseos em aplicações cirúrgicas. As nanopartículas de prata e hidroxiapatita foram incorporadas em

compósitos de matriz polimérica apresentando atividade antimicrobiana contra cinco espécies patogênicas: *Escherichia coli*, *Staphylococcus aureus*, *Staphylococcus* spp., *Bacillus cereus*, e *Candida albicans*.

Já no estudo de Xie et al. (2014), nanopartículas de hidroxiapatita decorada com prata foram sintetizadas com a finalidade de revestir superfícies de implantes metálicos para melhorar a osteoindutividade e propriedades antibacterianas contra cepas de *Staphylococcus epidermidis* and *Escherichia coli*, com a finalidade de ser implantado na engenharia de ossos.

Xiong et al. (2016) sintetizaram nanofios de hidroxiapatita decorada com prata para a preparação de um novo tipo de papel inorgânico altamente flexível, com propriedade antibacteriana para *Escherichia coli* e *Staphylococcus aureus*, como um biomaterial funcional promissor.

Por sua vez, Gutierrez et al. (2018) sintetizaram nanopartículas monodispersas de prata com ouro, altamente reativas, com tamanhos menores que 5 nm. Neste estudo foi demonstrado alta atividade antifúngica frente a espécies de *Candida*: *C. albicans*, *C. parapsilosis*, *C. krusei*, *C. glabrata*, e *C. guilliermondii*, a fim de tratar doenças fúngicas em humanos, animais e plantas, ou para revestir superfícies cirúrgicas. No entanto, sua aplicabilidade é interferida pelo alto custo do ouro.

Vale ressaltar que nos estudos citados não houve avaliação da toxicidade dos compostos visando uma possível biomédica. Modelos invertebrados possibilitam demonstrar diferentes respostas toxicológicas ou inflamatórias sem empregar mamíferos (IGNASIAK; MAXWELL, 2017; POYNTON et al., 2018; TANGUAY, 2018).

O modelo em *Galleria mellonella* (Lepidoptera - Pyralidae) tem sido utilizada como um modelo essencial para mostrar a virulência de diferentes patógenos devido à alta similaridade de resposta imune e níveis de toxicidade entre mamíferos, afim de sintetizar novos tratamentos medicamentosos com alta aplicabilidade (IGNASIAK; MAXWELL, 2017).

## 2- OBJETIVOS

Testar atividade antifúngica e toxicidade de nanocompósitos Ag-HAP, sintetizado em única etapa assistida por micro-ondas.

### 2.1 Objetivos específicos:

- Avaliar as características de cristalinidade, morfologia e distribuição controlada dos nanocompósitos.
- Determinar a atividade antifúngica, por microdiluição, frente à *Candida albicans, C. glabrata, C. krusei, C. parapsilosis stricto sensu* e *C. tropicalis*,;
- Determinar a toxicidade, *in vivo,* dos nanocompósitos sintetizados em modelo invertebrado *Galleria mellonella.*

**CAPÍTULO 2**

## Revised Manuscript

# One-Pot Synthesis and Antifungal Activity of Non-Toxic Silver-Hydroxyapatite Nanocomposites against *Candida* Species

*Bianca Gottardo,* [†] *Thiago H. Lemes,* [†] Gabriela *Byzynski,* [‡] *Mario H. Paziani,* [§] *Márcia R. V. Z. Kress,* [§] *Margarete T. G. de Almeida,* [‡] *and Diogo P. Volanti* [*,†]

† Institute of Biosciences, Humanities, and Exact Sciences, São Paulo State University (Unesp), R. Cristóvão Colombo 2265, São José do Rio Preto, SP15054-000, Brazil

‡ São José do Rio Preto Medical School (Famerp), Av. Brigadeiro Faria Lima 5416, São José do Rio Preto, SP 15090-000, Brazil

§ School of Pharmaceutical Sciences of Ribeirão Preto, University of São Paulo (USP), Av. do Café s/n, Ribeirão Preto, SP 14040-903, Brazil

KEYWORDS: nanostructured materials, one-pot synthesis, *Candida,* minimum inhibitory concentration, mycoses.

ABSTRACT: The impact of fungal diseases and the battle to antimicrobial agents by pathogenic fungi has developed actually as a main worldwide healthcare challenge. Here, the antifungal performance of silver-hydroxyapatite (Ag-HAP) nanocomposites (NCs) with different Ag concentrations synthesized by the one-pot microwave-assisted solvothermal method were evaluated against sensitive and resistant *Candida* species. Antifungal studies were conducted by microdilution method – protocol from the National Committee for Clinical Laboratory Standards. The main inhibitory effect was seen to Ag4%-HAP against *Candida krusei*, with minimum inhibitory concentration (MIC) of 31.2µg/mL, followed by *Candida parapsilosis stricto sensu* (62.5 µg/mL), *Candida tropicalis,* (62.5 µg/mL), *Candida glabrata* (125 µg/mL) and *Candida albicans* (125 µg/mL). Furthermore, the toxicity assay was made *in vivo* model using *Galleria mellonella* larvae. The test was executed by bathing or inoculating with the same NCs concentration used in the previous microdilution tests. All NCs no-showed any toxicity for both approaches. The specific antifungal activity demonstrates that NCs act efficiently against species of *Candida*. These results show a potential antifungal application for well-designed nanostructured Ag-HAP composites.

## 1. INTRODUCTION

Nowadays, several fungi diseases become a major problem of public health,[1–3] contributing to the increased morbidity and mortality in immunocompromised or immunocompetent patients.[4,5] During infection, high doses of antifungal drugs are used and are not always effective, leading to antifungal resistance rates.[6–9] Among all fungal infections, *Candida* species represents the most reported organism for colonization or infection in the skin, respiratory and genitourinary tract.[10–13] Considering the pathogenic species, *Candida albicans* is the most important, with several virulence factors[14] and different pattern of antimicrobial susceptibility to azoles.[15–17] It is broadly dispersed in nature and act as usual saprophytic elements of the typical human microbiota. In the nosocomial setting, this species represents the most common microorganism of fungal infection.[18,19] Nevertheless, recently, other non-*albicans Candida* (NAC) species are emerging as agents of nosocomial infectious diseases, as clinical isolates worldwide.[20] The most common NAC species of clinical importance are *Candida krusei, Candida glabrata*, *Candida tropicalis*, *Candida parapsilosis* Sensu Stricto, and *Candida guilliermondii.*[4,21,22] Some species, *Candida glabrata* and *Candida krusei,* presents the inherent antifungal resistance to azoles, especially fluconazole and itraconazole, responsible for treatment failure.[23,24] Silver (Ag) nanoparticles (NPs) can reach cells better than microparticles. The reduced size of AgNPs[25,26] contributes to the application in antimicrobial control of bacterial and fungal diseases.[27–31] In addition, these compounds can be associated to hydroxyapatite (HAP, $[Ca_5(PO_4)_3(OH)]$), a natural component of bones and teeth structure. The biocompatibility feature of HAP make this NP an excellent alternative for nano-biotechnology and nanomedicine.[25,33] Others

works combined Ag with HAP for application in bone tissue engineering to improve antimicrobial effects, getting high biocompatibility and low rejection.[33–35] Ag-loaded HAP nanowires presents high biocompatibility and antibacterial activity.[25] Au, Ag and Au-Ag nanoreactors synthesized in reverse micelle presents antifungal activity against *Candida* species.[36] However, few studies report *in vivo* toxicity tests on nanomaterials with antifungal or antibacterial activities. An interesting alternative model is the greater wax moth *Galleria mellonella* (Lepidoptera: Pyralidae), [37] an insect whose larva has been used in several kinds of research as a model to show virulence of different pathogens, drug treatments and toxicity levels of new compounds.[37–39] The goal of this work was to perform the one-pot microwave-assisted solvothermal (MAS) synthesis of non-toxic Ag-HAP NCs with controlled morphology, homogeneous size distribution, and different Ag weight percentage. The antifungal activity of the nanomaterials was tested using triphenyl tetrazolium chloride in American Type Culture Collection (ATCC) strains of *Candida albicans, Candida glabrata*, *Candida krusei, Candida parapsilosis* Sensu Stricto, and *Candida tropicalis* for potential biomedical application. The *in vivo* toxicity tests of NCs synthesized in this work were performed in *Galleria mellonella* larvae by both the contact by bath and the injection of the diluted NCs samples in the larvae. Finally, this work contributes into the knowledge of biophysiochemical interactions at the nano–bio interface between Ag-HAP NCs and *Candida* species.

## 2. EXPERIMENTAL SECTION

**2.1. Materials.** Calcium nitrate tetrahydrate ($Ca(NO_3)_2.4H_2O$, 99% purity), silver nitrate ($AgNO_3$, 99% purity), ethanol ($CH_3CH_2OH$, ≥98% purity), sodium hydroxide (NaOH, ≥98% purity), triphenyl tetrazolium chloride ($C_{19}H_{15}ClN_4$, 95% purity), sodium dihydrogen phosphate dihydrate ($NaH_2PO_4.2H_2O$, ≥ 99.0% purity), RPMI-1640 medium were purchased from Sigma-Aldrich. Besides, dimethyl sulfoxide ($C_2H_6OS$, 99.9% purity) was obtained from Synth. Finally, the aqueous solutions were prepared with Milli-Q® ultrapure water to reach a resistivity of 18.2 MΩ.cm (at 25°C). **2.2. Syntheses of Ag-HAP NCs.** The Ag-HAP NCs were prepared by a one-pot microwave-assisted solvothermal (MAS) adapted from Xiong et al.[25] For this purpose, $Ca(NO_3)_2.4H_2O$ (2.88 mmol) and $AgNO_3$ (0.145 mmol) were dissolved in 20 mL of distilled water and 12 mL of ethanol, under stirring. After that, 20 mL of aqueous solution containing 0.025 mol of NaOH was added to the mixture. After stirring for 30 min, 10 mL of 0.3 mol $L^{-1}$ $NaH_2PO_4.2H_2O$ solution was added to the mix. The resulted solution was inserted in Teflon reactor to perform the one-pot synthesis, during 60 minutes and 140°C by MAS method in the microwave apparatus (2.5 GHz and 800 W).[40] Finally, the powders precipitated from the precursor solution were washed four times with deionized water and centrifuged at 7,000 rpm until pH = 7 and subsequently dried at 90 °C overnight. The Ag-HAP NCs were prepared with different Ag content labeled as Ag2%-HAP, Ag4%-HAP, and Ag8%-HAP. The pure HAP was obtained as the same method described for Ag-HAP NCs. In addition, nanostructured metallic Ag obtained in our previous work,[41] was used as a control to compare the antifungal and toxicological tests. **2.3. Ag-HAP NCs Characterization.** The Ag-HAPs NCs were characterized by X-ray diffraction

(XRD) with Rigaku equipment, model MiniFlex 300 (Cu Kα radiation, λ = 1.5418 Å) with 2θ from 10° to 80°, at 2° $min^{-1}$. The crystallite sizes of the samples were estimated by Scherrer equation to the full width at half maximum (FWHM) of the (211), (112), and (002) peaks. The morphology and size of Ag-HAP NCs were characterized by field emission scanning electron microscopy (FE-SEM) with JEOL microscopy, model JSM 6701F and transmission electron microscope (TEM, FEI TTECNAI $G^2$ S-TWIN) operated at an accelerating voltage of 200 kV. Energy-dispersive X-ray spectroscopy (EDS) was also collected in a JEOL microscope, model SEM 6310 to evaluate the Ag distribution in the Ag-HAP NCs. Also, conductive carbon tapes were used for FE-SEM/EDX analyses The Fourier transformation infrared (FTIR) spectra were obtained in a Perkin Elmer spectrophotometer, model Spectrum Two. The optical images with magnification power (400x) were obtained in a Bioval binocular light microscope, model L2000. **2.4. Antifungal Susceptibility Testing.** The antifungal activity of Ag-HAP NCs, pure HAP, and pure Ag was performed in triplicate (100 µL of RPMI with inoculum and 100 µL of NCs solution), according to the instruction of CLSI M27-A3 method,[42] for *Candida albicans* (ATCC 10231), *Candida. glabrata* (ATCC 2001), *C. krusei* (ATCC 40147), *C. parapsilosis* Sensu Stricto (ATCC 22019), and *C. tropicalis* (ATCC 13803), with some modifications considering the antifungal drug. The isolates were kept at 37°C in RPMI broth media culture after overnight incubation. Each inoculum was adjusted according to the protocol, considering the turbidity of 0.5 MacFarland standard tube. In a 96-well microtitre plates (TPP, Switzerland), 100 µL of RPMI with fungal inoculum was added into each well. The NCs samples were dissolved in 10% dimethyl sulfoxide solution (DMSO) and added

into each well in the final concentration ranging from 250 to 1.95 µg/mL. The plates were incubated for 24 h, and after, 20 µg/mL of triphenyl tetrazolium (TTC) solution (20 µg/mL) was added into each well to evaluate the fungal cell viability after NCs contact. The surviving yeasts reduced the TTC to red formazan (1,3,5-triphenylformazan), and the non-surviving yeasts have shown no color. Several studies presented the TTC as a visual colorimetric method[43,44] to measure the antimicrobial potential because is an redox indicator used to see the difference between metabolically active tissues from non-active tissues, and cell viability. The mechanism is based on the enzymatic reduction of 1,3,5-triphenyltetrazolium (colorless) to 1,3,5-triphenylformazan (colored). In alive cells, the activity of dehydrogenases is in all oxidation mechanism even in microorganisms.[45,46] **2.5. *In vivo* Toxicity Test.** The toxicity of all Ag-HAP NCs samples were tested in *G. mellonella in vivo* model.[47] Groups of 10 sixth-instar larvae of *G. mellonella* (weight in the range of 250 to 350 mg each) were used in each methodology. For toxicity test both methods were performed, larvae bathing in Ag-HAP NCs samples and artificial inoculation into de larvae hemolymph. For the first, the larvae were submitted to bathing during two seconds in each Ag-HAP NCs samples solution (500 µg/mL) to evaluate the superficial toxicity. The artificial inculation was performed by injecting 5 µL of Ag-HAP NCs sample solutions (500 µg/mL) with a Hamilton 10 µL 7000.5KH syringe into the larva's hemocel through the last right proleg. The quaternary ammonium and DMSO solutions were used as positive and negative controls, respectively. The larvae were incubated at 28°C, deprived of feed and direct illumination. Every 12 hours, the larvae were removed from the pre-pupae to

delay their metamorphosis. Survival was monitored every 24 hours and the statistical analyses were performed by the *Log-rank* (Mantel-Cox) method.

## 3. RESULTS AND DISCUSSION

XRD patterns showed in Figure 1 confirm the crystalline phase is hexagonal HAP (JCPDS n$^{o}$ 86-740). The Ag diffraction peaks (111), (200), (220) and (311) relating to cubic structure appears in all NCs samples agreeing to JCPDS n$^{o}$ 4-783. As the Ag content in the NCs increases, the (111) intensity plane becomes higher. Xiong et al.[25] showed a one-step solvothermal of the Ag NP-decorated HAP synthesis at 180°C for 24 h. Here, the XRD results showed in Figure 1 indicate that crystalline Ag-HAP NCs were obtained at 140 °C for 1 hour by the one-pot MAS. Also, the crystallite sizes of the samples were calculated from the XRD information by applying the Scherrer parameters,[48] to the FWHM average of the (211), (112), and (002) peaks. The crystallite sizes determined by this method were 17.90, 17.98, 18.96 and 19.70 nm for the HAP, Ag2%-HAP, Ag4%-HAP, and Ag8%-HAP, respectively. These results indicate that the crystallite size of the NCs increases subtly as the silver concentration in HAP increases.

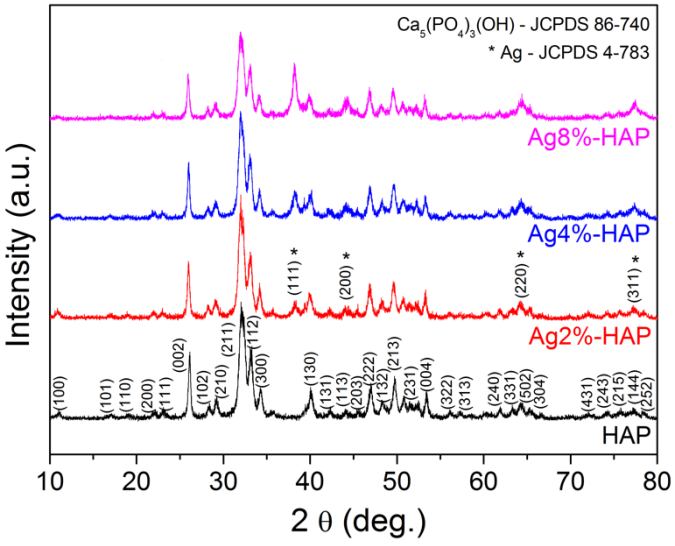


**Figure 1. XRD patterns of the Ag-HAP NCs prepared by the one-pot microwave-assisted solvothermal process with different Ag content.**

Figure 2 shows the images collected by transmission electron microscopy (TEM). The Figure 2a indicates that the dispersed and homogeneous HAP structures have rod-like morphologies of around length 62.7 nm and width 17.4 nm. The Figures 2b-c show that Ag NPs are homogeneously dispersed over HAP in the Ag2%-HAP and Ag4%-HAP samples, respectively. On the other hand, the Ag NPs are more agglomerated in the Ag8%-HAP NC. At higher magnification, it is possible to verify that the HAP nanoparticles are polycrystalline (Figure 2e) and in the inset of this image it is possible to index the interplanar distance of 0.344 nm referring to the (002) crystallographic plane of the HAP by high-resolution (HR) TEM. In the Figures 2f-h (Ag2%-HAP, Ag4%-HAP, 8% Ag-HAP, in that order), spherical Ag NPs have approximately size of 16.2, 18.6 and 20.2 nm in diameter can be indexed by (111) plane corresponding to an interplanar distance of 0.23 nm, according to its inset figures. Thus, as the concentration of Ag increases, there is an increase in the number of nanoparticles and also in the size of the Ag NPs. The SAED analyzes (Figures 2i-1) show that HAP and other NCs obtained are polycrystalline. It is possible to index the crystallography plans (002), (112), (130), (222), (213), (004) and (311) for the HAP in the Figure 2i. In the samples with different concentrations of Ag, the plans (201), (212), (220) and (231) correspondent to HAP appears for the sample of 2% Ag (Figure 2j). The plans (202), (130), (221) and (134) confirm the HAP phase for the Ag4%-HAP sample (Figure 2k), and the plans (111), (210), (302) and (132), also of HAP structure appear in the composition of Ag8%-HAP (Figure 2l). Interestingly, it is not possible to index any diffraction pattern for Ag NPs. This fact can be explained

by the small size of the Ag NPs and also by the high dispersion of the NCs that does not favor the appearance of measurable signal by SAED.

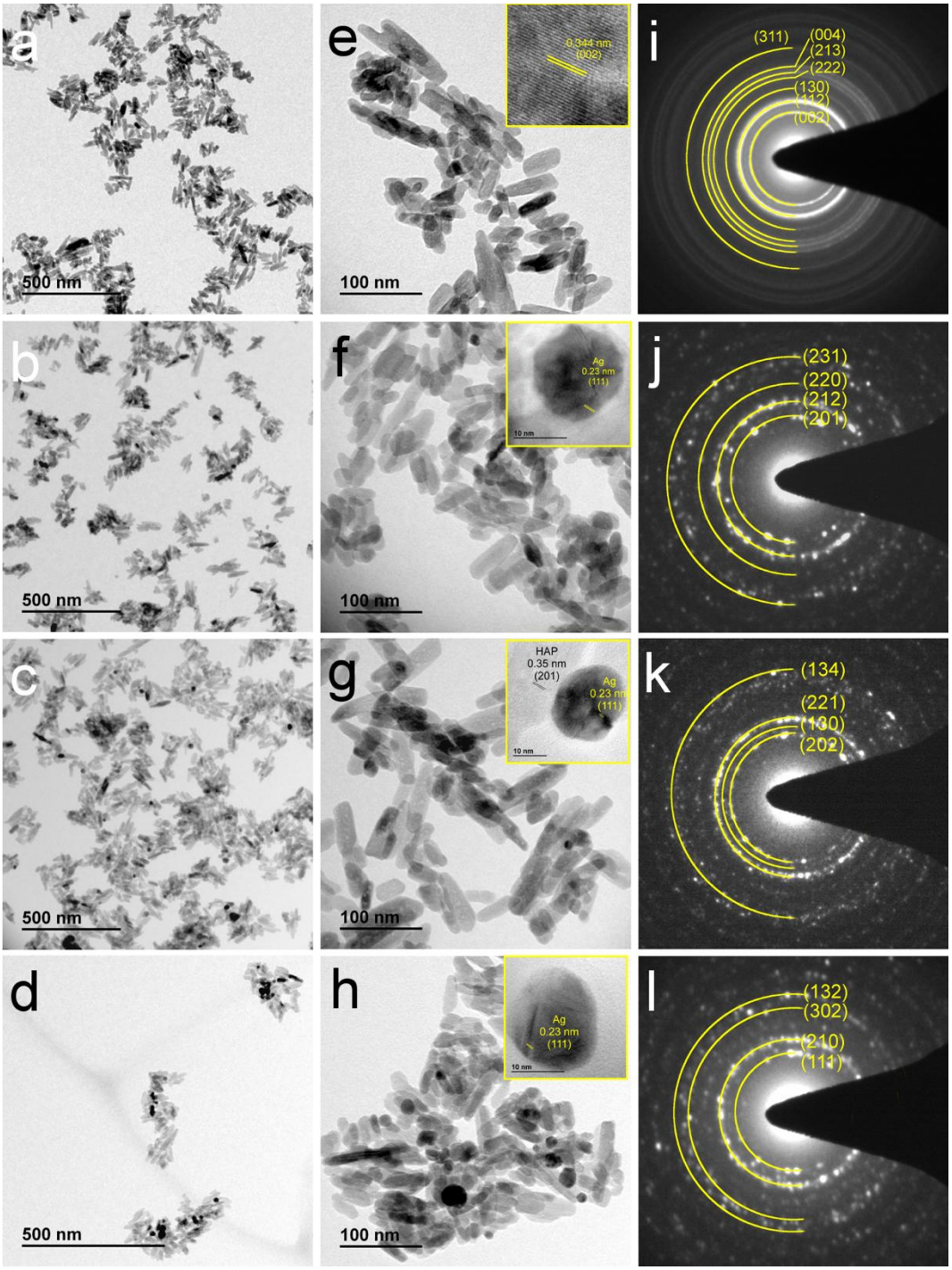


**Figure 2: Low magnification TEM images (a–d), high magnification TEM images (e–h), and the SAED patterns images (i–l) of the HAP, Ag2%-HAP, Ag4%-HAP, and Ag8%-HAP, in that order. The inset in the high magnification TEM figures shows HRTEM images.**

Figures 3a-c shows FE-SEM images of Ag2%-HAP, Ag4%-HAP, and Ag8%-HAP agglomerations, respectively. Besides, the Figures 3d-f shows the EDS x-ray mapping of Ag of the Ag2%-HAP, Ag4%-HAP, and Ag8%-HAP, respectively. This analysis allowed to confirm that Ag particles are uniformly dispersed on the surface of samples. The EDS mapping diagram of O, Ca and P elements in NC agglomerations were presented in Figures S1-S3, and the analysis confirms a uniform distribution of these elements on the samples. Moreover, the Ag quantity in Ag-HAP NCs was estimated by EDS spectra (Figure 3g), and atomic percentages of C, O, Na, P, Ca, and Ag were presented in Table 1. The expected Ag amounts in the nanocomposites are less than their nominal value. This fact can be explained by the loss of Ag ions during the MAS synthesis and wash centrifugation step. The amount of C present in the analysis is due to the use of carbon tape to leave conductive samples during FE-SEM analysis. Also, the EDX analysis shows that weight ratio Ca/P is about 2.3. This value is consistent with the stoichiometric ratio of these two elements in the hydroxyapatite structure (5 mols Ca (40.078 g x $mol^{-1}$): 3 mols P (30.974 g x $mol^{-1}$). Previous studies,[28,49] have reported that Ag-doping HAP results to their inclusion in the HAP lattice by exchanging $Ca^{2+}$ ions. Consequently, the pattern molar ratio Ca/P of the materials altered, like this the stoichiometry of the HAP was lost. The atomic ratio Ca/P increase from 2.23 for HAP at 2.34 and 2.35 for Ag2%-HAP and Ag4%-HAP, respectively. Thus, this result indicates that at these concentrations Ag does not tend to substitute Ca, remaining on the surface of HAP. On the other hand, the 8% sample showed a small decrease in the Ca/P ratio which may be the result of the exchange of a small amount of Ca atoms by Ag. In addition, due to the high ratio of surface

area to volume, the nanostructured HAP have a considerable fraction of Ca and P clusters can be predictable as compared to HAP in the microscale.[50]

**Table 1. Ag-HAPs NCs chemical composition obtained through EDS analysis. The elements were presented in atomic percentage in the resulted compound.**

| | C | O | Na | P | Ca | Ag |
|---|---|---|---|---|---|---|
| **HAP** | 13.88 | 39.91 | 1.60 | 13.09 | 29.26 | - |
| **Ag2%-HAP** | 16.66 | 35.59 | 1.45 | 12.59 | 29.51 | 1.61 |
| **Ag4%-HAP** | 14.37 | 36.88 | 1.23 | 12.69 | 29.84 | 3.52 |
| **Ag8%-HAP** | 13.09 | 39.62 | 1.73 | 11.78 | 26.09 | 6.63 |

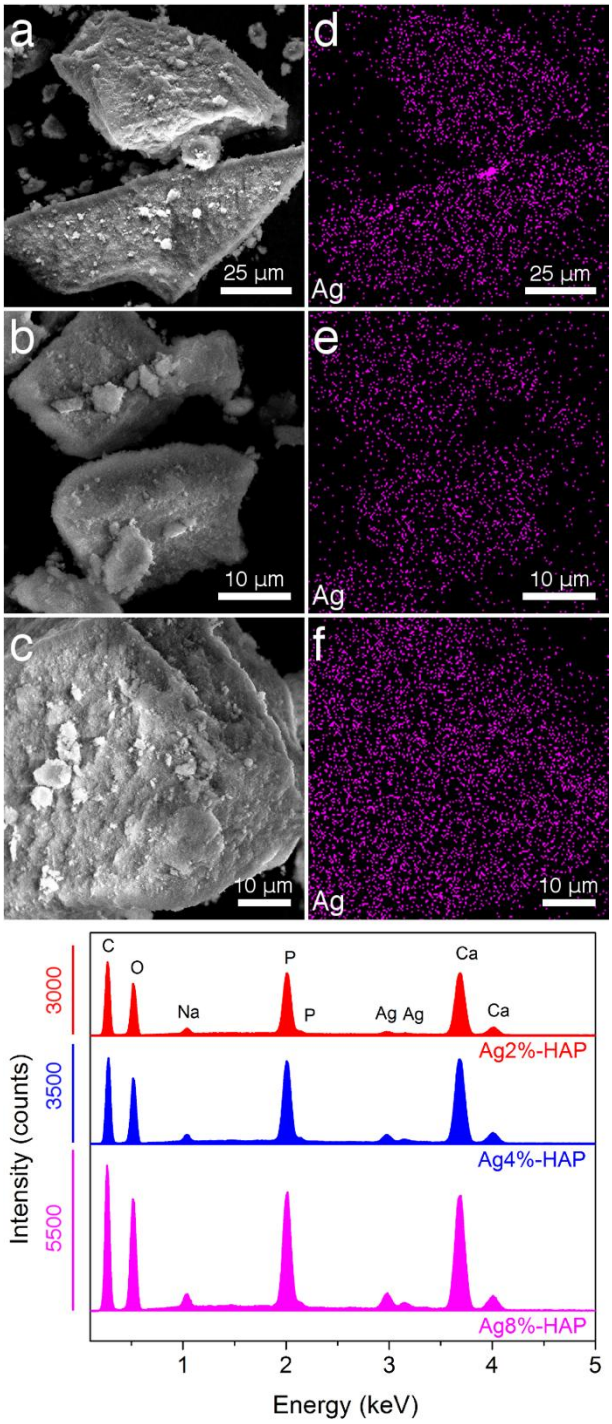


**Figure 3: EDX distribution diagram analysis of Ag element of a) Ag2%-HAP, b) Ag4%-HAP, c) Ag8%-HAP agglomerations, Figures 3d-f shows the EDS x-ray mapping of Ag of the Ag2%-HAP, Ag4%-HAP, and Ag8%-HAP agglomerations, respectively, and g) EDS spectra of Ag-HAPs NCs.**

FTIR spectra (Figure 4) did not show significance difference between molecules on HAP and Ag-HAP NCs surfaces. The bands at 565 and 604 $cm^{-1}$ are

attributed to the O−P−O bond (bending mode) of the $PO_4^{3-}$. The typical absorption bands at 961, 1025, and 1086 $cm^{-1}$ are correlated to the symmetric and asymmetric stretching modes of $PO_4^{3-}$ anion. The absorption peaks at 1414 and 1456 $cm^{-1}$ are ascribed to the C−O bending mode characteristics of $CO_2$ surface adsorption on Ag-HAP NCs.

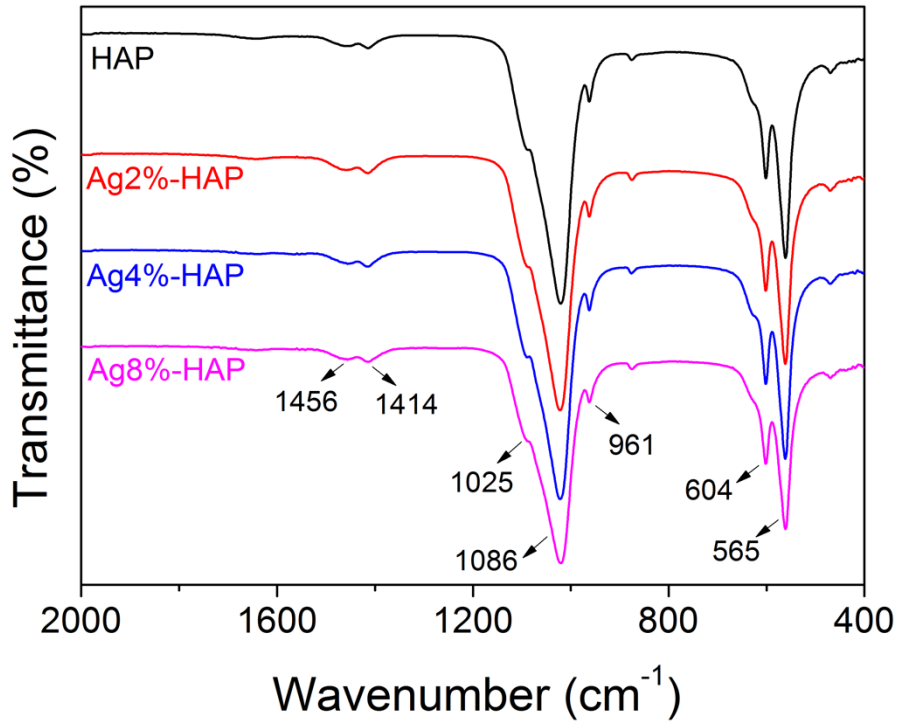


**Figure 4: FTIR spectra of HAP and Ag-HAP NCs.**

The antifungal susceptibility testing of Ag-HAP NCs as well as the pure Ag are showed in Table 2. The results of Ag 4%-HAP and Ag 8%-HAP were more effective in the inhibitory action than the pure Ag and Ag 2%-HAP, independent of the *Candida* species. Although Ag2%-HAP did not show the best action, *Candida krusei* was inhibited with MIC of 125 µg/mL. This event was important because this species is resistant to azole drugs and difficult to control, very common in systemic diseases, present in 73% of global fungal infection.[51] Interesting, the compound with higher Ag concentration (Ag8%-HAP) did not

exhibit the best antifungal activity in comparison to the others. In Figure 6, the region 1 indicate the fungal grow control, yet region 2 show DMSO 10% solubility test. In the region 3 is possible view sterility control RPMI broth. The regions 4 to 9 indicate NCs within fungal culture, and region 10 represent the MIC of Ag-HAP NCs that kill the yeasts. These results can be explained because pure Ag NPs under high concentrations, tend to agglomerate, which could limit its action.[25] The HAP did not show any antifungal activity, but when associated with Ag, the synergistic effect happened because antifungal potential was improved. It is well known that, HAP is highly biocompatible, and it is an essential carrier of metallic NPs, such as Ag.[52] The best activity of the compounds was observed against *Candida krusei* (Figure 5), *Candida tropicalis* (Figure S6), and *Candida parapsilosis stricto sensu* (Figure S7), while the poorest, for *Candida albicans* (Figure S4) and *Candida glabrata* (Figure S5). The present investigation detected different result of NPs of Ag antifungal activity against *Candida krusei,* prior described by Szweda et al.[53] The Ag association with HAP can be an alternative against this species because it is difficult to control and should present specific structural targets for Ag-HAP.[54] In addition, the reason why Ag NPs presents an antifungal activity is because of their effective contact with the fungal which destroy the cell membrane and inhibits the common growth process due to the damage and loss of membrane structure, and due to the creation of pores that may led to the cell annihilation.[55] Ag NPs exercises an antifungal activity against *C. albicans* and others fungi because of the production and accumulation of free hydroxyl radicals (•OH) and reactive oxygen species (ROS) inside the microorganism cells, which regulates and induces the cell death through release of cytochrome c, mitochondrial

dysfunctional apoptosis, nuclear fragmentation, the metacaspases activation, and DNA destruction.[56]

**Table 2.** MIC results (µg/mL) of the tested NCs against five species of *Candida*.

| *Candida* Species | NCs samples | | | |
|---|---|---|---|---|
| | Ag2%-HAP | Ag4%-HAP | Ag8%-HAP | Pure Ag |
| *C. albicans* | 250 | 125 | 250 | 250 |
| *C. glabrata* | 250 | 125 | 125 | 250 |
| *C. krusei* | 125 | 31.25 | 31.25 | 62.5 |
| *C. parapsilosis Sensu Stricto* | 250 | 62.5 | 62.5 | 125 |
| *C. tropicalis* | 250 | 62.5 | 62.5 | 125 |

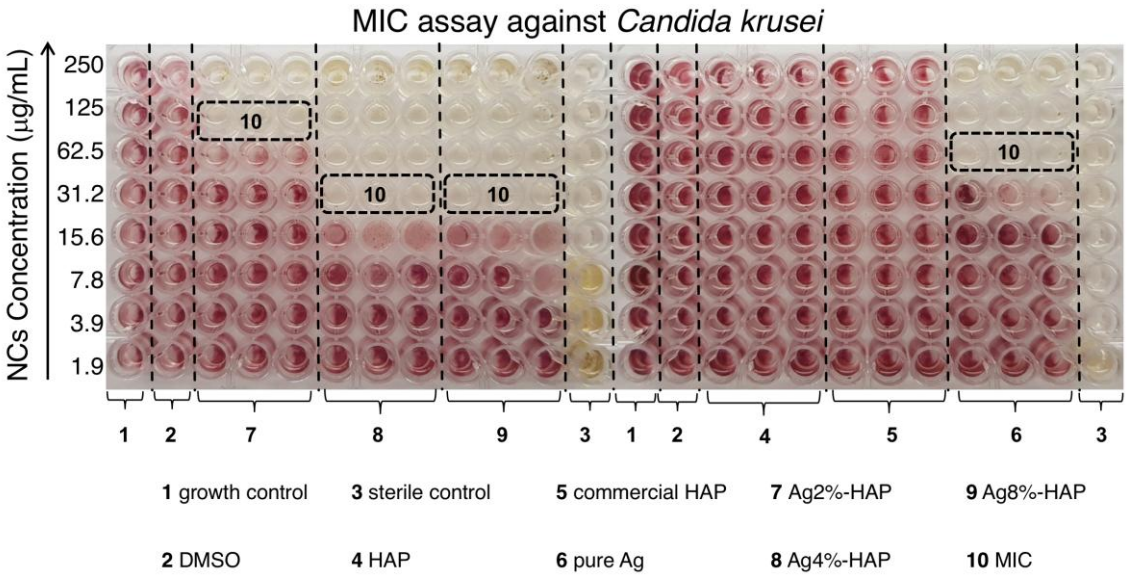


**Figure 5. Picture of antifungal susceptibility testing of Ag-HAP NCs and controls against *Candida krusei*. Viability test with triphenyl tetrazolium (TTC) solution. NCs, nanocomposites; DMSO, dimethyl sulphoxyde; HAP, hydroxyapatite; Ag, silver;MIC, minimal inhibitory concentration.**

The analysis of optical light microscopy, showed the attraction between the fungal cell with Ag-HAP NCs, event that did not occur with pure Ag (Figure 6). In relation with nanoscale, news phenomenon appears, the electrostatic forces are high than the gravity forces and it could explain this attraction,[57] due to the differences in charge between cell wall and hydroxyapatite. [58,59] The mechanism of action has been ascribed to the interaction between the positive charge on Ag ion and the negative charge from oxygenated functional groups on microbial cell (fungi possess cell walls made of glucans, chitin, mannans, and glycoproteins).[60] In addiction the pure Ag did not show any attraction with yeasts because the HAP is smaller than the pure Ag, and the forces are not so strong. Moreover, it is important to consider that the ATCC strains, here analyzed, normally present different pattern of antimicrobial susceptibility than clinical strains, since the last one are exposed to metabolic stress, with change of phenotype.[61] The similar inhibitory activity of Ag4%-HAP and Ag8%-HAP samples was observed for *Candida parapsilosis stricto sensu* and *Candida tropicalis.* Once more an interesting result, because both fungal species are responsible to severe infectious disease and can form biofilm, resulting in microbial communities of difficult control.

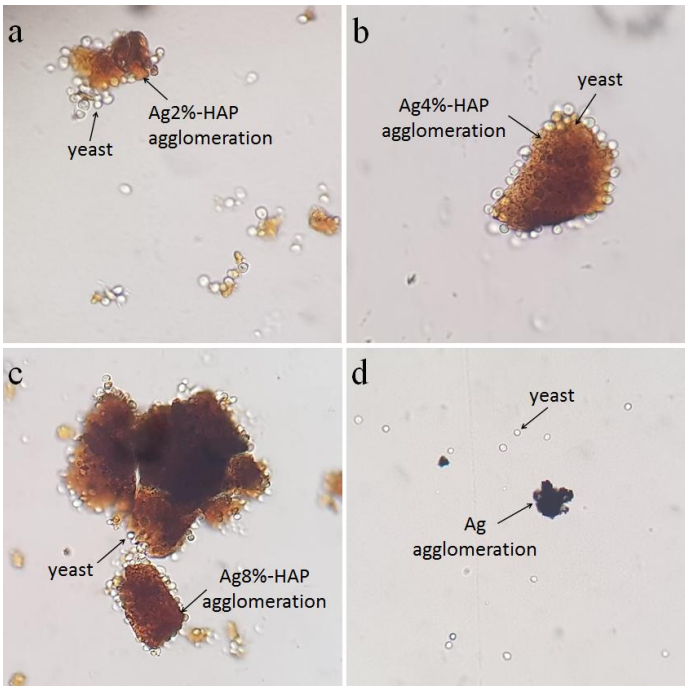


**Figure 6: (a-c) Images of yeast linked to Ag2%-HAP, Ag4%-HAP and Ag8%-HAP NCs, respectively; d) pure Ag sample not attracted by the yeast. The images were obtained by light microscope magnification power (400X).**

The toxicity of each compound was tested in the *in vivo* model *Galleria mellonella*. This model system has similarities with the immune and toxicity response of the mammals. The larvae hematocytes work as phagocyte and release proteins which are similar to mammalian anti-body).[37–39] The initial test starts with 10 larvae, the 100% alive organisms. When the experiment was finished, the number of larvae alive/ dead was measured to get the final number/percentage of survival. The samples Ag2%-HAP, Ag4%-HAP, and Ag8%-HAP were non-toxic with statistical significance ($P < 0.05$) as well as the non-associated HAP and pure Ag ($P < 0.05$). In general, $P < 0.05$ or lower means that we are assuming a probability of only 5% that the difference found in the *in vivo* toxicity is not true, although statistically it has been demonstrated.

The lower the value of *P*, the lower the probability of this happening. It could be explained because the phagocytosis by macrophage is declined face to nanoparticles sized less than 260nm, and the infection response do not appear in an important intensity.[62] Among these compounds, neither the bathing nor the injection of the samples was able to kill the larvae, except the positive control, ammonium quaternary (toxic compound), which killed all larvae in 24 hours after the bath and 48 hours after injection (Figure 7). Also, high performance in antifungal tests and low toxicity was possible probably due to the excellent dispersion of Ag NPs in the matrix, the sized very reduced and HAP biocompatibility.

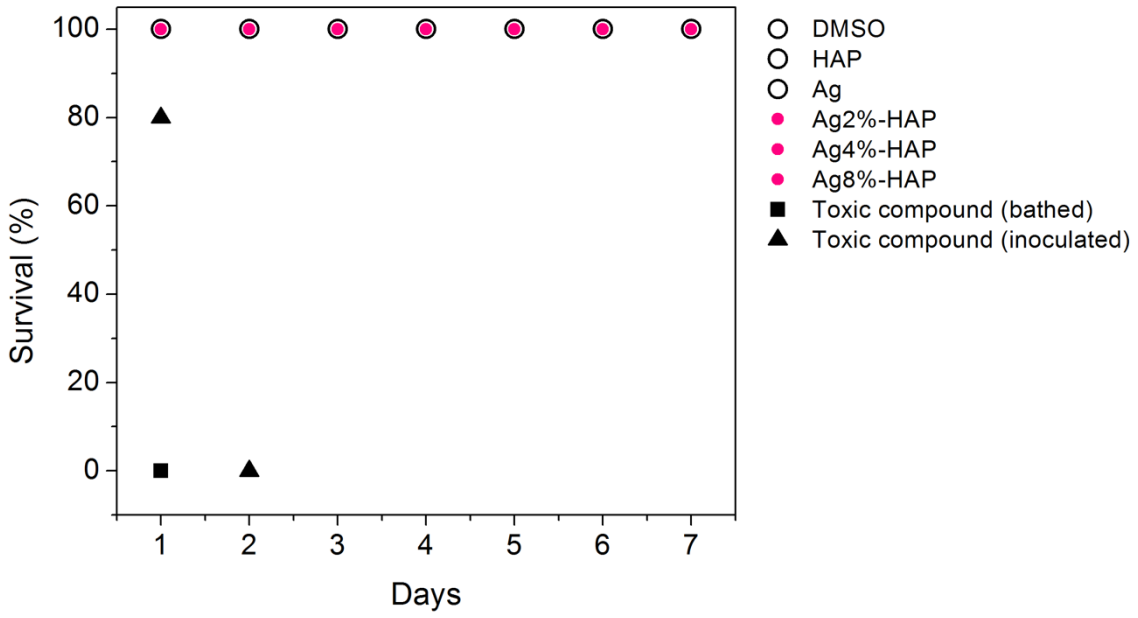


**Figure 7. Graphic representation of toxicity test of NCs and controls in *Galleria mellonella.* The survival percentage of *Galleria mellonella* when inoculated and bathed with toxic quaternary ammonium and innocuous DMSO solution (*P* < 0.05).**

## 4. CONCLUSIONS

In summary, this study shows a one-pot MAS synthesis of non-toxic Ag-HAP NCs with different weight concentrations of Ag NPs against five *Candida* species. According to these results, the HAP nanorods works as a non-toxic matrix to attract the fungi. On the other hand, the Ag NPs acts as fungicide material which can be encompassed by the microorganisms. Interestingly, the synthetized NCs have shown a smallest MIC values against *Candida krusei*, and also good activity against other species of *Candida*. The remarkable antifungal performance shown by the NCs could be attributed to the electrostatic interaction force between Ag NPs and fungal cell wall surface, with specificity for some receptors. Ag NPs can interact with microorganism organelles, leading to the protein synthesis reduction, rupture of the cell wall and membrane cell, then consequently inhibiting the cellular budding. The *in vivo* non-toxic effect can be due to well-dispersed Ag NPs (in low concentration) on HAP nanorods matrix, that protect the host against cell damage. These data open new nanotechnological approaches to Ag-HAP-based NCs to control fungal diseases without causing toxicity damages.

## ASSOCIATED CONTENT

**Supporting Information**. EDS distribution diagram analysis of O, Ca and P elements of NCs and images of MIC test against others tested *Candidas* species (PDF).

AUTHOR INFORMATION

Corresponding Author

E-mail: diogo.volanti@unesp.br

ORCID

Diogo P. Volanti: 0000-0001-9315-9392

Author Contributions. The authors declare no competing financial interest. The manuscript was written through contributions of all authors. All authors have given approval to the final version of the manuscript.

ACKNOWLEDGMENT

The authors are thankful to the financial support of the São Paulo Research Foundation – FAPESP (grants 2017/01267-1 and 2015/04511-5), National Council for Scientific and Technological Development – CNPq (grants 444926/2014-3 and 402287/2013-4), National Council for the Improvement of Higher Education (CAPES), SISNANO/MCTI, FINEP and Embrapa AgroNano research network. The FE-SEM facilities were provided by the Nanotechnology National Laboratory for Agriculture (LNNA), Embrapa Instrumentation, São Carlos, São Paulo, Brazil. TEM facilities were provided by LCE/DEMa/UFSCar. We acknowledge the Multi-user Laboratory (LMU) at São Jose do Rio Preto (Famerp).

REFERENCES

(1) Hakki, M.; Staab, J. F.; Marr, K. A. Emergence of a Candida krusei isolate with reduced susceptibility to caspofungin during therapy. *Antimicrob. Agents Chemother.* **2006**, *50* (7), 2522–2524 DOI: 10.1128/AAC.00148-06.

(2) Isenmann, Michael Schwarz, Bettina, R. Characteristics of Infection with Candida Species inPatients with Necrotizing Pancreatitis. *World J. Surg.* **2002**, *26* (3), 372–376 DOI: 10.1007/s00268-001-0146-9.

(3) Kollef, M.; Micek, S.; Hampton, N.; Doherty, J. A.; Kumar, A. Septic shock attributed to Candida infection: Importance of empiric therapy and source control. *Clin. Infect. Dis.* **2012**, *54* (12), 1739–1746 DOI: 10.1093/cid/cis305.

(4) Sadeghi, G.; Ebrahimi-Rad, M.; Mousavi, S. F.; Shams-Ghahfarokhi, M.; Razzaghi-Abyaneh, M. Emergence of non- Candida albicans species: Epidemiology, phylogeny and fluconazole susceptibility profile. *J. Mycol. Med.* **2018**, *28* (1), 51–58 DOI: 10.1016/j.mycmed.2017.12.008.

(5) Al-Dorzi, H. M.; Sakkijha, H.; Khan, R.; Aldabbagh, T.; Toledo, A.; Ntinika, P.; Al Johani, S. M.; Arabi, Y. M. Invasive Candidiasis in Critically Ill Patients: A Prospective Cohort Study in Two Tertiary Care Centers. *J. Intensive Care Med.* **2018**, 088506661876783 DOI: 10.1177/0885066618767835.

(6) Parkinson, T.; Falconer, D. J.; Hitchcock, C. A. Fluconazole resistance due to energy-dependent drug efflux in Candida glabrata. *Antimicrob. Agents Chemother.* **1995**, *39* (8), 1696–1699 DOI: 10.1128/AAC.39.8.1696.

(7) Ramage, G. Investigation of multidrug efflux pumps in relation to fluconazole resistance in Candida albicans biofilms. *J. Antimicrob. Chemother.* **2002**, *49* (6), 973–980 DOI: 10.1093/jac/dkf049.

(8) Bhattacharya, S.; Fries, B. C. Enhanced Efflux Pump Activity in Old Candida glabrata Cells. *Antimicrob. Agents Chemother.* **2018**, *62* (3), e02227-17 DOI: 10.1128/AAC.02227-17.

(9) Vipulanandan, G.; Herrera, M.; Wiederhold, N. P.; Li, X.; Mintz, J.; Wickes, B. L.; Kadosh, D. Dynamics of Mixed–Candida Species Biofilms in Response to Antifungals. *J. Dent. Res.* **2018**, *97* (1), 91–98 DOI: 10.1177/0022034517729351.

(10) Bertini, A.; De Bernardis, F.; Hensgens, L. A. M.; Sandini, S.; Senesi, S.; Tavanti, A. Comparison of Candida parapsilosis, Candida orthopsilosis, and Candida metapsilosis adhesive properties and pathogenicity. *Int. J. Med. Microbiol.* **2013**, *303* (2), 98–103 DOI: 10.1016/j.ijmm.2012.12.006.

(11) Merz, W. G.; Karp, J. E.; Schron, D.; Saral, R. Increased incidence of fungemia caused by _Candida krusei. *J Clin.Microbiol.* **1986**, *24* (0095–1137 (Print)), 581–584.

(12) Davidson, L.; Netea, M. G.; Kullberg, B. J. Patient Susceptibility to Candidiasis—A Potential for Adjunctive Immunotherapy. *J. Fungi* **2018**, *4* (1), 9 DOI: 10.3390/jof4010009.

(13) Pappas, P. G.; Lionakis, M. S.; Arendrup, M. C.; Ostrosky-Zeichner, L.; Kullberg, B. J. Invasive candidiasis. *Nat. Rev. Dis. Prim.* **2018**, *4* (May), 18026 DOI: 10.1038/nrdp.2018.26.

(14) Mayer, F. L.; Wilson, D.; Hube, B. Candida albicans pathogenicity mechanisms. *Virulence* **2013**, *4* (2), 119–128 DOI:

doi.org/10.4161/viru.22913.

(15) Khandelwal, N. K.; Chauhan, N.; Sarkar, P.; Esquivel, B. D.; Coccetti, P.; Singh, A.; Coste, A. T.; Gupta, M.; Sanglard, D.; White, T. C.; et al. Azole resistance in a Candida albicans mutant lacking the ABC transporter CDR6/ROA1 depends on TOR signaling. *J. Biol. Chem.* **2018**, *293* (2), 412–432 DOI: 10.1074/jbc.M117.807032.

(16) Panariello, B. H. D.; Klein, M. I.; Mima, E. G. D. O.; Pavarina, A. C. Fluconazole impacts the extracellular matrix of fluconazole-susceptible and -resistant Candida albicans and Candida glabrata biofilms. *J. Oral Microbiol.* **2018**, *10* (1), 1476644 DOI: 10.1080/20002297.2018.1476644.

(17) Moron, L. S.; Cabrera, E. C. Detection of azole resistance and ERG11 point mutations in Candida albicans isolates from tertiary hospitals in the Philippines. *Cream J.* **2018**, *8* (April), 298–305 DOI: 10.5943/cream/8/3/1.

(18) Karacaer, Z.; Oncul, O.; Turhan, V.; Gorenek, L.; Ozyurt, M. A surveillance of nosocomial candida infections: epidemiology and influences on mortalty in intensive care units. *Pan Afr. Med. J.* **2014**, *19*, 1–9 DOI: 10.11604/pamj.2014.19.398.4960.

(19) Hsu, J.-F.; Lai, M.-Y.; Lee, C.-W.; Chu, S.-M.; Wu, I.-H.; Huang, H.-R.; Lee, I.-T.; Chiang, M.-C.; Fu, R.-H.; Tsai, M.-H. Comparison of the incidence, clinical features and outcomes of invasive candidiasis in children and neonates. *BMC Infect. Dis.* **2018**, *18* (1), 194 DOI: 10.1186/s12879-018-3100-2.

(20) Clancy, C. J.; Nguyen, M. H. Diagnosing Invasive Candidiasis. *J. Clin. Microbiol.* **2018**, *56* (5), e01909-17 DOI: 10.1128/JCM.01909-17.

(21) Kaur, R.; Dhakad, M. S.; Goyal, R.; Kumar, R. Emergence of non-

albicans Candida species and antifungal resistance in intensive care unit patients. *Asian Pac. J. Trop. Biomed.* **2016**, *6* (5), 455–460 DOI: 10.1016/j.apjtb.2015.12.019.

(22) Mäkinen, A.; Nawaz, A.; Mäkitie, A.; Meurman, J. H. Role of non- albicans Candida and Candida albicans in oral squamous cell cancer patients. *J. Oral Maxillofac. Surg.* **2018** DOI: 10.1016/j.joms.2018.06.012.

(23) Whaley, S. G.; Berkow, E. L.; Rybak, J. M.; Nishimoto, A. T.; Barker, K. S.; Rogers, P. D. Azole Antifungal Resistance in Candida albicans and Emerging Non-albicans Candida Species. *Front. Microbiol.* **2017**, *7* (JAN), 1–12 DOI: 10.3389/fmicb.2016.02173.

(24) Castanheira, M. Fungemia Surveillance in Denmark Demonstrates Emergence of Non- albicans Candida Species and Higher Antifungal Usage and Resistence than in other Nations. *J. Clin. Microbiol.* **2018**, *56* (4), 1–4 DOI: https://doi.org/10.1128/JCM .01907-17.

(25) Xiong, Z.-C.; Zhu, Y.-J.; Chen, F.-F.; Sun, T.-W.; Shen, Y.-Q. One-Step Synthesis of Silver Nanoparticle-Decorated Hydroxyapatite Nanowires for the Construction of Highly Flexible Free-Standing Paper with High Antibacterial Activity. *Chem. - A Eur. J.* **2016**, *22* (32), 11093–11093 DOI: 10.1002/chem.201602799.

(26) González, B.; Colilla, M.; Díez, J.; Pedraza, D.; Guembe, M.; Izquierdo-Barba, I.; Vallet-Regí, M. Mesoporous silica nanoparticles decorated with polycationic dendrimers for infection treatment. *Acta Biomater.* **2018**, *68*, 261–271 DOI: 10.1016/j.actbio.2017.12.041.

(27) Khatami, M.; Sharifi, I.; Nobre, M. A. L.; Zafarnia, N.; Aflatoonian, M. R. Waste-grass-mediated green synthesis of silver nanoparticles and

evaluation of their anticancer, antifungal and antibacterial activity. *Green Chem. Lett. Rev.* **2018**, *11* (2), 125–134 DOI: 10.1080/17518253.2018.1444797.

(28) Popa, C. L.; Ciobanu, C. S.; Voicu, G.; Vasile, E.; Chifiriuc, M. C.; Iconaru, S. L.; Predoi, D. Influence of Thermal Treatment on the Antimicrobial Activity of Silver-Doped Biological Apatite. *Nanoscale Res. Lett.* **2015**, *10* (1), 502 DOI: 10.1186/s11671-015-1211-x.

(29) Marcato, P. D.; Durán, M.; Huber, S. C.; Rai, M.; Melo, P. S.; Alves, O. L.; Durán, N. Biogenic Silver Nanoparticles and its Antifungal Activity as a New Topical Transungual Drug. *J. Nano Res.* **2012**, *20*, 99–107 DOI: 10.4028/www.scientific.net/JNanoR.20.99.

(30) Kou, L.; Bhutia, Y. D.; Yao, Q.; He, Z.; Sun, J.; Ganapathy, V. Transporter-guided delivery of nanoparticles to improve drug permeation across cellular barriers and drug exposure to selective cell types. *Front. Pharmacol.* **2018**, *9* (JAN), 1–16 DOI: 10.3389/fphar.2018.00027.

(31) Volova, T. G.; Shumilova, A. A.; Shidlovskiy, I. P.; Nikolaeva, E. D.; Sukovatiy, A. G.; Vasiliev, A. D.; Shishatskaya, E. I. Antibacterial properties of films of cellulose composites with silver nanoparticles and antibiotics. *Polym. Test.* **2018**, *65* (November 2017), 54–68 DOI: 10.1016/j.polymertesting.2017.10.023.

(32) Zeng, Y.; Yan, Y.; Yan, H.; Liu, C.; Li, P.; Dong, P.; Zhao, Y.; Chen, J. 3D printing of hydroxyapatite scaffolds with good mechanical and biocompatible properties by digital light processing. *J. Mater. Sci.* **2018**, *53* (9), 6291–6301 DOI: 10.1007/s10853-018-1992-2.

(33) Saravanan, S.; Nethala, S.; Pattnaik, S.; Tripathi, A.; Moorthi, A.;

Selvamurugan, N. Preparation, characterization and antimicrobial activity of a bio-composite scaffold containing chitosan/nano-hydroxyapatite/nano-silver for bone tissue engineering. *Int. J. Biol. Macromol.* **2011**, *49* (2), 188–193 DOI: 10.1016/j.ijbiomac.2011.04.010.

(34) Mocanu, A.; Furtos, G.; Rapuntean, S.; Horovitz, O.; Flore, C.; Garbo, C.; Danisteanu, A.; Rapuntean, G.; Prejmerean, C.; Tomoaia-Cotisel, M. Synthesis; characterization and antimicrobial effects of composites based on multi-substituted hydroxyapatite and silver nanoparticles. *Appl. Surf. Sci.* **2014**, *298*, 225–235 DOI: 10.1016/j.apsusc.2014.01.166.

(35) Xie, C.-M.; Lu, X.; Wang, K.-F.; Meng, F.-Z.; Jiang, O.; Zhang, H.-P.; Zhi, W.; Fang, L.-M. Silver Nanoparticles and Growth Factors Incorporated Hydroxyapatite Coatings on Metallic Implant Surfaces for Enhancement of Osteoinductivity and Antibacterial Properties. *ACS Appl. Mater. Interfaces* **2014**, *6* (11), 8580–8589 DOI: 10.1021/am501428e.

(36) Gutiérrez, J. A.; Caballero, S.; Díaz, L. A.; Guerrero, M. A.; Ruiz, J.; Ortiz, C. C. High Antifungal Activity against Candida Species of Monometallic and Bimetallic Nanoparticles Synthesized in Nanoreactors. *ACS Biomater. Sci. Eng.* **2018**, *4* (2), 647–653 DOI: 10.1021/acsbiomaterials.7b00511.

(37) Cook, S. M.; McArthur, J. D. Developing Galleria mellonella as a model host for human pathogens. *Virulence* **2013**, *4* (5), 350–353 DOI: 10.4161/viru.25240.

(38) Brennan, M. Correlation between virulence of Candida albicans mutants in mice and Galleria mellonella larvae. *FEMS Immunol. Med. Microbiol.* **2002**, *34* (2), 153–157 DOI: 10.1016/S0928-8244(02)00374-7.

(39) Ignasiak, K.; Maxwell, A. Galleria mellonella (greater wax moth) larvae as a model for antibiotic susceptibility testing and acute toxicity trials. *BMC Res. Notes.* **2017**, *10* (1), 428 DOI: 10.1186/s13104-017-2757-8.

(40) Elson Longo da Silva; José Arana Varela; Dawy Keyson de Araújo Almeida; Diogo Paschoalini Volanti. Microwave Aided Device for Hydrothermal Synthesis of Nanostructured Oxides, Particularly Obtaining Particles of Metal Oxides, Comprises Container, in which Hydrothermal Reaction Takes Place, and Lid for Container. BR200815393-A2, 2010.

(41) Sá, B. S.; Zito, C. A.; Perfecto, T. M.; Volanti, D. P. Production of Nanostructured Silver from Waste Radiographic Films Using a Microwave-Assisted Hydrothermal Method. *J. Sustain. Metall.* **2018**, *4* (3), 407–411 DOI: 10.1007/s40831-018-0187-z.

(42) CLSI. *Clinical and Laboratory Standards Institute: Método de Referência para Testes de Diluição em Caldo para Determinação da Sensibilidade de Leveduras à Terapia Antifúngica : Norma Aprovada – Segunda Edição*; 2012; Vol. 22.

(43) Vostálová, J.; Cukr, M.; Zálešák, B.; Lichnovská, R.; Ulrichová, J.; Rajnochová Svobodová, A. Comparison of various methods to analyse toxic effects in human skin explants: Rediscovery of TTC assay. *J. Photochem. Photobiol. B Biol.* **2018** DOI: 10.1016/j.jphotobiol.2017.12.011.

(44) Berridge, M. V.; Herst, P. M.; Tan, A. S. Tetrazolium dyes as tools in cell biology: New insights into their cellular reduction. In *Biotechnology Annual Review*; 2005; pp 127–152.

(45) Praveen-Kumar; Tarafdar, J. C. 2,3,5-Triphenyltetrazolium chloride (TTC)

as electron acceptor of culturable soil bacteria, fungi and actinomycetes. *Biol. Fertil. Soils* **2003** DOI: 10.1007/s00374-003-0600-y.

(46) Saviano, A. M.; Lourenço, F. R. Rapid microbiological methods (RMMs) for evaluating the activity of cephalosporin antibiotics employing triphenyltetrazolium chloride. *Talanta* **2018**, *185*, 520–527 DOI: 10.1016/j.talanta.2018.04.020.

(47) Renwick, J.; Daly, P.; Reeves, E. P.; Kavanagh, K. Susceptibility of Larvae of Galleria mellonella to Infection by Aspergillus fumigatus is Dependent upon Stage of Conidial Germination. *Mycopathologia* **2006**, *161* (6), 377–384 DOI: 10.1007/s11046-006-0021-1.

(48) Patterson, A. L. The Scherrer Formula for X-Ray Particle Size Determination. *Phys. Rev.* **1939**, *56* (10), 978–982 DOI: 10.1103/PhysRev.56.978.

(49) Dorozhkin, S. Calcium Orthophosphate-Containing Biocomposites and Hybrid Biomaterials for Biomedical Applications. *J. Funct. Biomater.* **2015**, *6* (3), 708–832 DOI: 10.3390/jfb6030708.

(50) Han, Y.; Wang, X.; Dai, H.; Li, S. Nanosize and Surface Charge Effects of Hydroxyapatite Nanoparticles on Red Blood Cell Suspensions. *ACS Appl. Mater. Interfaces* **2012**, *4* (9), 4616–4622 DOI: 10.1021/am300992x.

(51) Sanguinetti, M.; Posteraro, B.; Lass-Flörl, C. Antifungal drug resistance among Candida species: Mechanisms and clinical impact. *Mycoses* **2015**, *58* (S2), 2–13 DOI: 10.1111/myc.12330.

(52) Xiong, Z.-C.; Yang, Z.-Y.; Zhu, Y.-J.; Chen, F.-F.; Zhang, Y.-G.; Yang, R.-L. Ultralong Hydroxyapatite Nanowires-Based Paper Co-Loaded with Silver Nanoparticles and Antibiotic for Long-Term Antibacterial Benefit.

*ACS Appl. Mater. Interfaces* **2017**, *9* (27), 22212–22222 DOI: 10.1021/acsami.7b05208.

(53) Szweda, P.; Gucwa, K.; Kurzyk, E.; Romanowska, E.; Dzierżanowska-Fangrat, K.; Zielińska Jurek, A.; Kuś, P. M.; Milewski, S. Essential Oils, Silver Nanoparticles and Propolis as Alternative Agents Against Fluconazole Resistant Candida albicans, Candida glabrata and Candida krusei Clinical Isolates. *Indian J. Microbiol.* **2015**, *55* (2), 175–183 DOI: 10.1007/s12088-014-0508-2.

(54) Pfaller, M. A.; Diekema, D. J.; Gibbs, D. L.; Newell, V. A.; Nagy, E.; Dobiasova, S.; Rinaldi, M.; Barton, R.; Veselov, A. Candida krusei, a Multidrug-Resistant Opportunistic Fungal Pathogen: Geographic and Temporal Trends from the ARTEMIS DISK Antifungal Surveillance Program, 2001 to 2005. *J. Clin. Microbiol.* **2008**, *46* (2), 515–521 DOI: 10.1128/JCM.01915-07.

(55) Kim, K.-J.; Sung, W. S.; Suh, B. K.; Moon, S.-K.; Choi, J.-S.; Kim, J. G.; Lee, D. G. Antifungal activity and mode of action of silver nano-particles on Candida albicans. *BioMetals* **2009**, *22* (2), 235–242 DOI: 10.1007/s10534-008-9159-2.

(56) Hwang, I.; Lee, J.; Hwang, J. H.; Kim, K.-J.; Lee, D. G. Silver nanoparticles induce apoptotic cell death in Candida albicans through the increase of hydroxyl radicals. *FEBS J.* **2012**, *279* (7), 1327–1338 DOI: 10.1111/j.1742-4658.2012.08527.x.

(57) Min, Y.; Akbulut, M.; Kristiansen, K.; Golan, Y.; Israelachvili, J. The role of interparticle and external forces. 527–538.

(58) Bizerra, F. C.; Nakamura, C. V.; De Poersch, C.; Estivalet Svidzinski, T.

I.; Borsato Quesada, R. M.; Goldenberg, S.; Krieger, M. A.; Yamada-Ogatta, S. F. Characteristics of biofilm formation by Candida tropicalis and antifungal resistance. *FEMS Yeast Res.* **2008**, *8* (3), 442–450 DOI: 10.1111/j.1567-1364.2007.00347.x.

(59) Silva, S.; Negri, M.; Henriques, M.; Oliveira, R.; Williams, D. W.; Azeredo, J. Candida glabrata, Candida parapsilosis and Candida tropicalis : biology, epidemiology, pathogenicity and antifungal resistance. *FEMS Microbiol. Rev.* **2012**, *36* (2), 288–305 DOI: 10.1111/j.1574-6976.2011.00278.x.

(60) Bowman, S. M.; Free, S. J. The structure and synthesis of the fungal cell wall. *BioEssays* **2006**, *28* (8), 799–808 DOI: 10.1002/bies.20441.

(61) Baghdadi, E.; Khodavaisy, S.; Rezaie, S.; Abolghasem, S.; Kiasat, N.; Salehi, Z.; Sharifynia, S.; Aala, F. Antifungal Susceptibility Patterns of Candida Species Recovered from Endotracheal Tube in an Intensive Care Unit. *Adv. Med.* **2016**, *2016*, 1–6 DOI: 10.1155/2016/9242031.

(62) Azarmi, S.; Roa, W. H.; Löbenberg, R. Targeted delivery of nanoparticles for the treatment of lung diseases. *Adv. Drug Deliv. Rev.* **2008**, *60* (8), 863–875 DOI: 10.1016/j.addr.2007.11.006.

**Supporting Information Material**

# One-Pot Synthesis and Antifungal Activity of Non-Toxic Silver-Hydroxyapatite Nanocomposites against Candida Species

*Bianca Gottardo,* [†] *Thiago H. Lemes,* [†] Gabriela *Byzynski,* [‡] *Mario H. Paziani,* [§] *Márcia R. V. Z. Kress,* [§] *Margarete T. G. de Almeida,* [‡] *and Diogo P. Volanti* [*,†]

† Institute of Biosciences, Humanities, and Exact Sciences, São Paulo State University (Unesp), R. Cristóvão Colombo 2265, São José do Rio Preto, SP15054-000, Brazil

‡ São José do Rio Preto Medical School (Famerp), Av. Brigadeiro Faria Lima 5416, São José do Rio Preto, SP 15090-000, Brazil

§ School of Pharmaceutical Sciences of Ribeirão Preto, University of São Paulo (USP), Av. do Café s/n, Ribeirão Preto, SP 14040-903, Brazil

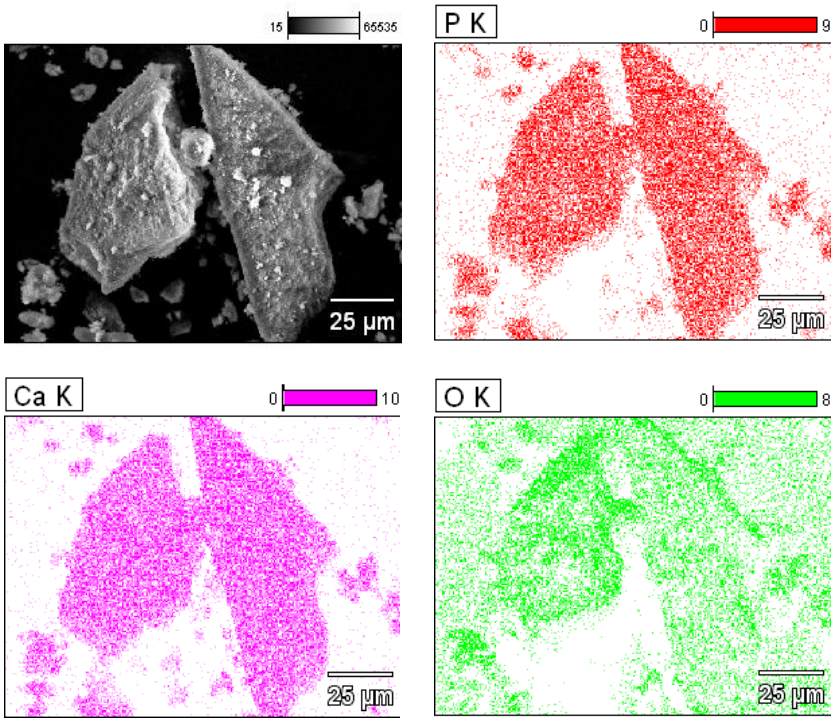


**Figure S1:** EDS distribution diagram analysis of O, Ca and P elements of Ag2%-HAP.

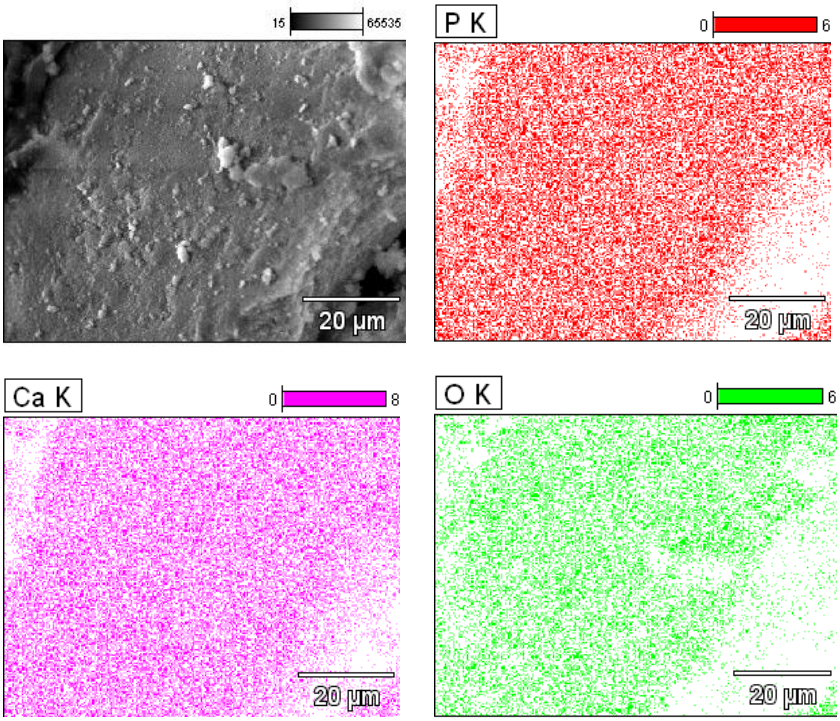


**Figure S2:** EDS distribution diagram analysis of O, Ca and P elements of Ag4%-HAP.

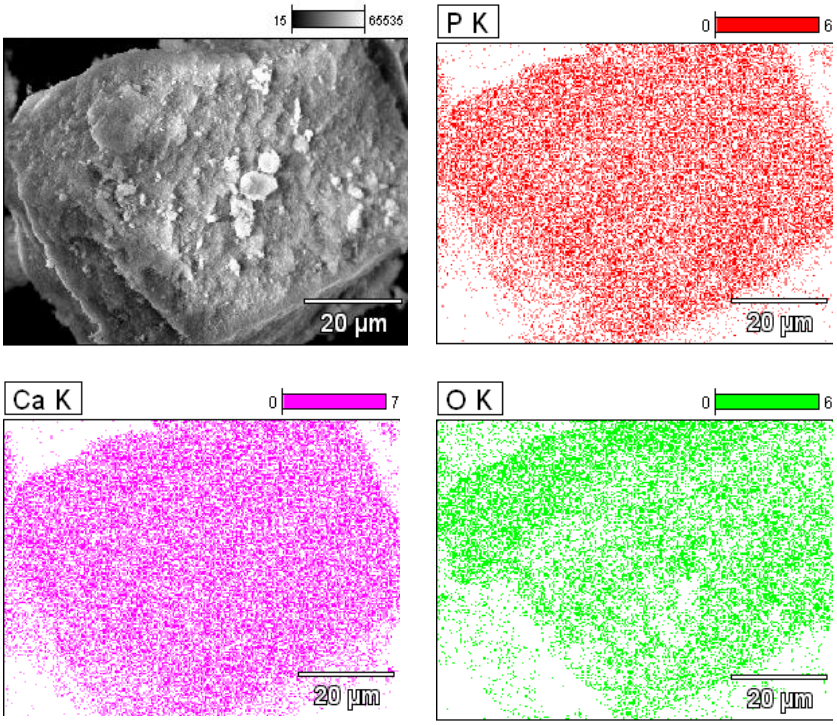


**Figure S3:** EDS distribution diagram analysis of O, Ca and P elements of Ag8%-HAP.

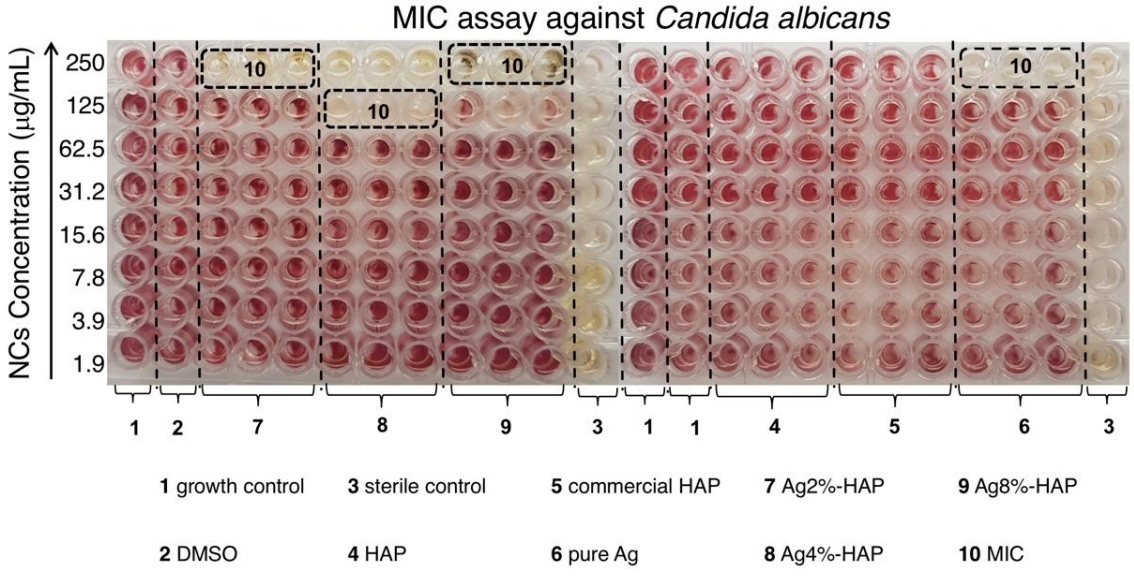


**Figure S4.** Picture of antifungal activity ( MIC assay) of NCs and controls against *Candida albicans*. Line 1: grow control; Line 2: DMSO 10% solubility test; Line 3: sterility control RPMI broth; Lines 4 to 9: NCs inside fungal culture; boxes 10: minimun inhibitory concentration of NCs that kill the yeasts.

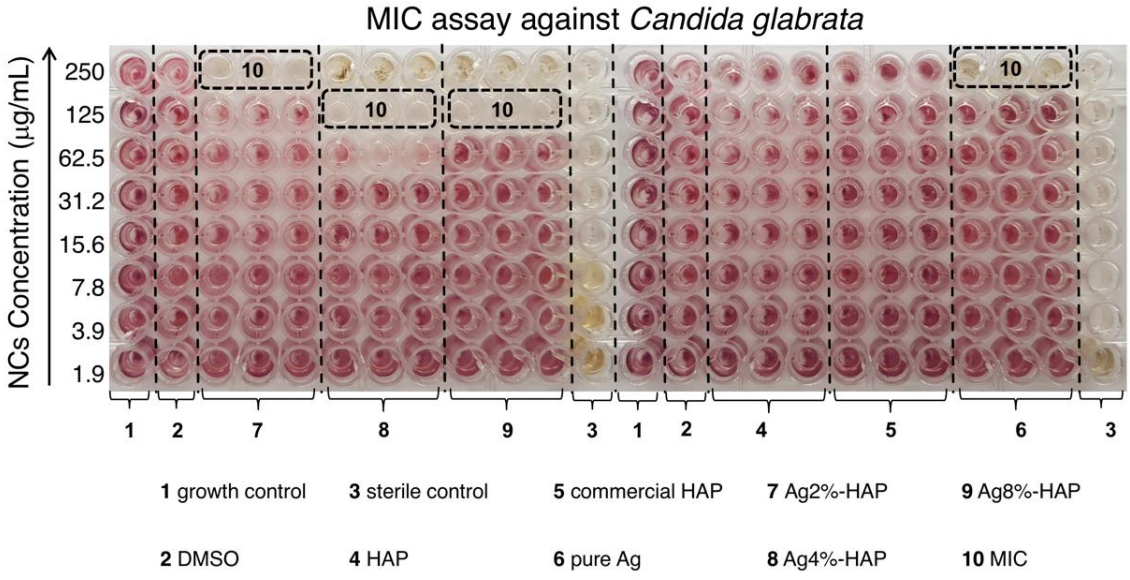


**Figure S5.** Picture of antifungal activity ( MIC assay) of NCs and controls against *Candida glabrata*. Line 1: grow control; Line 2: DMSO 10% solubility test; Line 3: sterility control RPMI broth; Lines 4 to 9: NCs inside fungal culture; boxes 10: minimun inhibitory concentration of NCs that kill the yeasts.

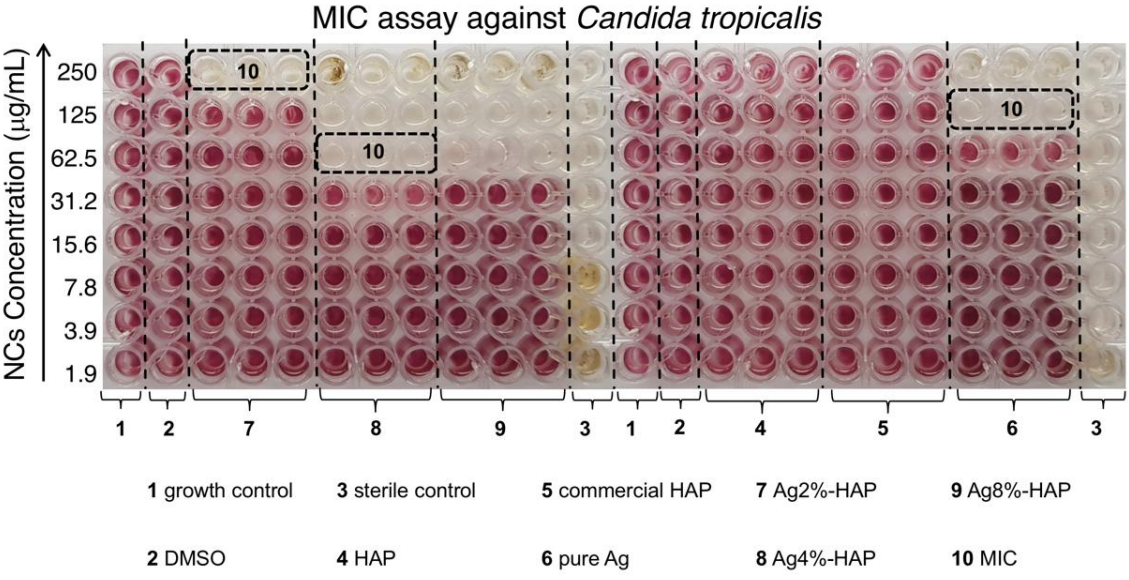


**Figure S6.** Picture of antifungal activity ( MIC assay) of NCs and controls against *Candida tropicalis*. Line 1: grow control; Line 2: DMSO 10% solubility test; Line 3: sterility control RPMI broth; Lines 4 to 9: NCs inside fungal culture; boxes 10: minimun inhibitory concentration of NCs that kill the yeasts.

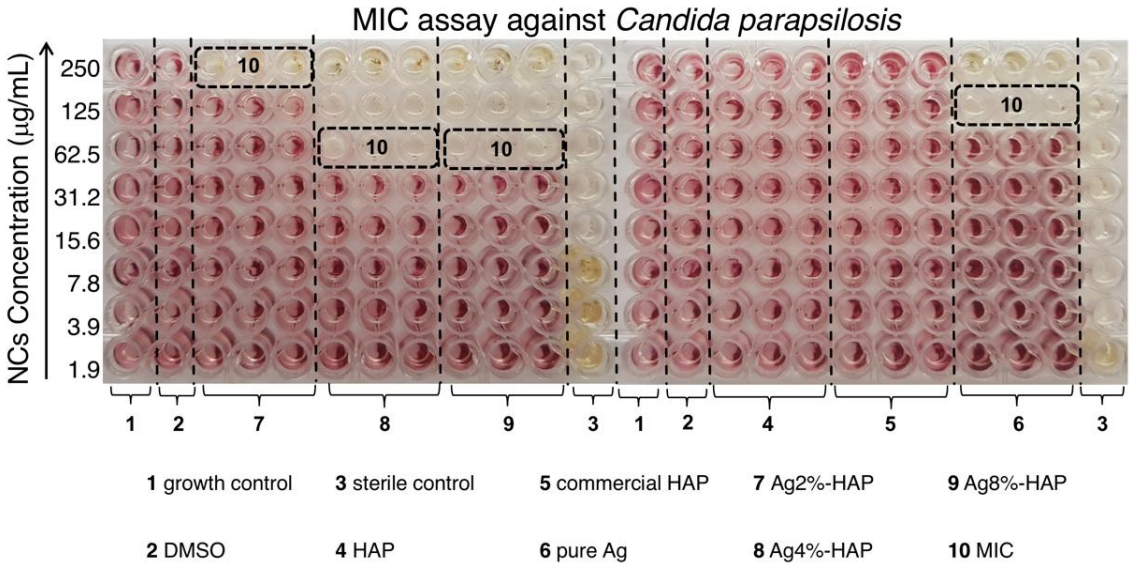


**Figure S7.** Picture of antifungal activity ( MIC assay) of NCs and controls against *Candida parapsilosis*. Line 1: grow control; Line 2: DMSO 10% solubility test; Line 3: sterility control RPMI broth; Lines 4 to 9: NCs inside fungal culture; boxes 10: minimun inhibitory concentration of NCs that kill the yeasts.

## CAPÍTULO 3

## 3- CONCLUSÃO

Este estudo mostra uma síntese em micro-ondas de nanocompósitos Ag-HAP não tóxicos com diferentes concentrações de peso de Ag NPs contra cinco cepas de *Candida.* De acordo com esses resultados, os nanobastões HAP funcionam como uma matriz não tóxica para atrair os fungos. Por outro lado, o Ag NPs atua como material fungicida que altera mecanismos biológicos dos microrganismos. Curiosamente, as amostras sintetizadas mostraram menores valores de concentração inibitória mínima contra *Candida krusei*, e também impostante atividade contra outras espécies de *Candida*. O notável desempenho antifúngico mostrado pelos NCs pode ser atribuído à força de interação eletrostática entre Ag NPs e superfície da parede celular fúngica, com especificidade para alguns receptores. Ags NPs podem interagir com microorganismos, levando à redução da síntese protéica, ruptura da parede celular e membrana celular, consequentemente inibindo o brotamento celular. O efeito não tóxico *in vivo* pode ser devido a disperssão homogênea de Ag NPs na matriz de nanobastões HAP, que protegem o hospedeiro contra danos celulares. Esses dados abrem novas abordagens nanotecnológicas para nanocompósitos de Ag-HAP para controlar doenças fúngicas sem causar danos por toxicidade.

## 4- REFERÊNCIAS


AARTHI, A. et al. Detection and degradation of leachate in groundwater using ag modified Fe3O4nanoparticle as sensor. **Journal of Molecular Liquids**, v. 252, p. 97–102, 2018.

BEYTH, N. et al. **Antimicrobial nanoparticles in restorative composites**. Second Edition ed. [s.l.] Elsevier Inc., 2017.

BONGOMIN, F. et al. Global and Multi-National Prevalence of Fungal Diseases—Estimate Precision. **Journal of Fungi**, v. 3, n. 4, p. 57, 2017.

BROWN, G. D. et al. Hidden killers: Human fungal infections. **Science Translational Medicine**, v. 4, n. 165, 2012.

CHERAGHI, M. et al. Heart targeted nanoliposomal/nanoparticles drug delivery: An updated review. **Biomedicine and Pharmacotherapy**, v. 86, p. 316–323, 2017.

CLEVELAND, A. A. et al. Declining incidence of candidemia and the shifting epidemiology of Candida resistance in two US metropolitan areas, 2008-2013: Results from population-based surveillance. **PLoS ONE**, v. 10, n. 3, p. 2008–2013, 2015.

DIEKEMA, D. et al. The changing epidemiology of healthcare-associated candidemia over three decades. **Diagnostic Microbiology and Infectious Disease**, v. 73, n. 1, p. 45–48, 2012.

FERNANDO, S.; GUNASEKARA, T.; HOLTON, J. Antimicrobial Nanoparticles: applications and mechanisms of action. **Sri Lankan Journal of Infectious Diseases**, v. 8, n. 1, p. 2, 2018.

FLOWERS, S. A. et al. Gain-of-function mutations in UPC2 are a frequent cause of ERG11 upregulation in azole-resistant clinical isolates of Candida albicans. **Eukaryotic Cell**, v. 11, n. 10, p. 1289–1299, 2012.

GONZÁLEZ, B. et al. Mesoporous silica nanoparticles decorated with polycationic dendrimers for infection treatment. **Acta Biomaterialia**, v. 68, p. 261–271, 2018.

HUFFNAGLE, G.; NOVERR, M. C. The emerging world of the fungal microbiome. **Fungal Microbiome**, v. 18, n. 9, p. 1199–1216, 2013.

IGNASIAK, K.; MAXWELL, A. Galleria mellonella (greater wax moth) larvae as a model for antibiotic susceptibility testing and acute toxicity trials. **BMC Research Notes**, v. 10, n. 1, p. 428, dez. 2017.

KATIYAR, S. K.; EDLIND, T. D. Identification and expression of multidrug

resistance-related ABC transporter genes in Candida krusei. **Medical Mycology**, v. 39, n. 1, p. 109–116, 2001.

KLINGSPOR, L. et al. Invasive Candida infections in surgical patients in intensive care units: A prospective, multicentre survey initiated by the European Confederation of Medical Mycology (ECMM) (2006-2008). **Clinical Microbiology and Infection**, v. 21, n. 1, p. 87.e1-87.e10, 2015.

KRISHNASAMY, L. et al. Molecular mechanisms of antifungal drug resistance in Candida species. **Journal of Clinical and Diagnostic Research**, v. 12, n. 9, p. DE01-DE06, 2018.

KULLBERG, B. J.; ARENDRUP, M. C. Invasive Candidiasis. **Journal of Physics A: Mathematical and Theoretical**, v. 44, n. 8, p. 85201, 25 fev. 2011.

KUMAR, V.; YADAV, S. K. Plant-mediated synthesis of silver and gold nanoparticles and their applications. **Journal of Chemical Technology and Biotechnology**, v. 84, n. 2, p. 151–157, 2009.

LAKSHMINARAYANAN, R. et al. Recent Advances in the Development of Antimicrobial Nanoparticles for Combating Resistant Pathogens. **Advanced Healthcare Materials**, v. 7, n. 13, p. 1–13, 2018.

LAMPING, E. et al. Abc1p is a multidrug efflux transporter that tips the balance in favor of innate azole resistance in Candida krusei. **Antimicrobial Agents and Chemotherapy**, v. 53, n. 2, p. 354–369, 2009.

LARA, H. H. et al. Synergistic antifungal effect of chitosan-stabilized selenium nanoparticles synthesized by pulsed laser ablation in liquids against Candida albicans biofilms. **International Journal of Nanomedicine**, v. 13, p. 2697–2708, 2018.

MAYER, F. L.; WILSON, D.; HUBE, B. Candida albicans pathogenicity mechanisms. **Virulence**, v. 4, n. 2, p. 119–128, 2013.

MOCANU, A. et al. Synthesis; Characterization and antimicrobial effects of composites based on multi-substituted hydroxyapatite and silver nanoparticles. **Applied Surface Science**, v. 298, p. 225–235, 2014.

NETEA, M. G. et al. Immune defence against Candida fungal infections. **Nature Reviews Immunology**, v. 15, n. 10, p. 630–642, 2015.

PAPPAS, P. G. et al. Invasive candidiasis. **Nature Reviews Disease Primers**, v. 4, p. 1445–1456, 2018.

PAUL, S.; MOYE-ROWLEY, W. S. Multidrug resistance in fungi: Regulation of transporter-encoding gene expression. **Frontiers in Physiology**, v. 5 APR, n. April, p. 1–14, 2014.

POYNTON, H. C. et al. The Toxicogenome of Hyalella azteca: A Model for

Sediment Ecotoxicology and Evolutionary Toxicology. **Environmental Science and Technology**, v. 52, n. 10, p. 6009–6022, 2018.

QIN, S. Y. et al. Drug self-delivery systems for cancer therapy. **Biomaterials**, v. 112, p. 234–247, 2017.

RICARDO, E. et al. In vivo and in vitro acquisition of resistance to voriconazole by Candida krusei. **Antimicrobial Agents and Chemotherapy**, v. 58, n. 8, p. 4604–4611, 2014.

SANTOS, G. C. D. O. et al. Candida infections and therapeutic strategies: Mechanisms of action for traditional and alternative agents. **Frontiers in Microbiology**, v. 9, n. JUL, p. 1–23, 2018.

SHARIFZADEH, A. et al. Oral microflora and their relation to risk factors in HIV+patients with oropharyngeal candidiasis. **Journal de Mycologie Medicale**, v. 23, n. 2, p. 105–112, 2013.

SPITZER, M.; ROBBINS, N.; WRIGHT, G. D. Combinatorial strategies for combating invasive fungal infections. **Virulence**, v. 8, n. 2, p. 169–185, 2017.

TANGUAY, R. L. The rise of zebrafish as a model for toxicology. **Toxicological Sciences**, v. 163, n. 1, p. 3–4, 2018.

WHALEY, S. G. et al. Azole antifungal resistance in Candida albicans and emerging non-albicans Candida Species. **Frontiers in Microbiology**, v. 7, n. JAN, p. 1–12, 2017.

XIAO, M. et al. Antifungal susceptibilities of Candida glabrata species complex, Candida krusei, Candida parapsilosis species complex and Candida tropicalis causing invasive candidiasis in China: 3 year national surveillance. **Journal of Antimicrobial Chemotherapy**, v. 70, n. 3, p. 802–810, 2015.

XIE, C. M. et al. Silver nanoparticles and growth factors incorporated hydroxyapatite coatings on metallic implant surfaces for enhancement of osteoinductivity and antibacterial properties. **ACS Applied Materials and Interfaces**, v. 6, n. 11, p. 8580–8589, 2014.

XIONG, Z. C. et al. One-Step Synthesis of Silver Nanoparticle-Decorated Hydroxyapatite Nanowires for the Construction of Highly Flexible Free-Standing Paper with High Antibacterial Activity. **Chemistry - A European Journal**, v. 22, n. 32, p. 11093, 2016.